Report
to

United States Army
Communications-Electronics Command
Research, Development and Engineering Center
Fort Monmouth, NJ 07703

of
NIST Special Tests of the Pipe Flows Produced by the Cheng Rotating Vane in Two Selected Elbow Configurations

G.E. Mattingly
T.T. Yeh
Fluid Flow Group
Process Measurements Division
Chemical Science and Technology Laboratory
National Institute of Standards and Technology
Gaithersburg, MD 20899

The purpose of these special tests was to measure the pipe flow effects produced by the Cheng Rotating Vane (CRV) installed in two prevalent piping configurations; the single elbow and the closely-coupled double elbows out-of-plane arrangement. These flow conditioning installations are intended to improve pipe flow conditions so that fluid meters installed downstream can measure satisfactorily. The flows studied here were done in 50 mm diameter pipe flowing water at a diametral Reynolds number of 10^5. The measurements were done using laser Doppler velocimetry (LDV); velocity measurement accuracies are quoted at $\pm 1\%$. The glass LDV test section was smoothly and concentrically joined to the stainless steel piping configurations so that the pipe flows described below can be assumed to occur when these fluid and flow conditions prevail.

Previous studies at NIST and elsewhere have shown that flow meter installation effects can significantly affect fluid meter performance. These NIST studies were arranged with special emphasis on the piping configuration effects: all flange joints preceding the test section were pinned to insure smooth, concentric alignments and marked so that precise rearrangements of the pipe work can be done, and all pipe joints were "O" ring sealed. Additionally, and most importantly, the pipe flows that enter each of the two elbow configurations described below was produced by the same long (72 D) straight piece of stainless steel, 50 mm diameter pipe. This pipe length produces, for these conditions, a fully developed turbulent pipeflow. In this way, the flows that exit the two elbow configurations described below are those produced only by these configurations.

The previous pipe flow measurement programs - done at NIST with the support of an industry-government consortium to study flow meter installation effects - produced extensive measurements for extended distances downstream of specific pipe elements. As requested, the studies described here for the single and double elbow configurations have been done only over 25-30 D of downstream pipe length.

The single elbow configuration studied both without and with the CRV conditioning element is shown in Sketch 1. The coordinate system is described in the caption. The closely-coupled double elbows out-of-plane configuration studied both without and with the CRV conditioning element is shown in Sketch 2. The coordinate system is described in the caption. Sketch 3 shows the closely-coupled double elbows out-of-plane configuration with the CRV installed, where the relationship is shown between the two coordinates systems selected to describe these results. Results are normalized using the inner pipe diameter, D, for lengths and the cross-sectionally averaged velocity, W_b for velocities.

Single Elbow Measurement Before CRV Installation

A summary of the LDV measurements made over about 25 D downstream of the single elbow is given in Figures 1-8, see Refrs. 1-2. In these, the time-averaged or mean axial velocity distributions denoted "Bogue and Metzner" are considered here to be the reference distributions for fully developed pipeflow, see Refr. 3. Of course, in fully developed pipeflow the mean velocity component in the radial and the azimuthal directions is zero. Therefore, the upward velocity component, V is zero in these conditions and this is labeled " Ideal" on the pertinent graphs. The measured root-mean-squared (rms) components of the turbulent velocities in the axial, w′ and vertical, v′ directions are plotted in comparison to the distributions measured by Laufer, for conditions similar to the NIST measurements, see Refr. 4. These distributions are plotted as solid lines and labeled "Laufer".

Figures 1-4 show NIST measurement results for the mean velocity components in the axial and vertical directions plotted versus the X and Y axes, respectively. For the axial components, results deviate from the Bogue and Metzner distribution by as much as 35% as measured 2.7 D downstream from the elbow exit to as little as 10% at the Z = 23.2 D location. Vertical components of mean velocity deviate by about 25% from ideal at the 2.7 D location to less than 5% at the 11.2 D location.

Figures 5-8 show rms components of the turbulent velocity in the axial and vertical directions plotted versus the X and Y axes, respectively. The characteristic features of these results are that both the axial and vertical components deviate qualitatively and quantitatively from the Laufer results at locations within about 6 D of the elbow exit. It is noted that the Reynolds number for the Laufer distributions is 41000. However, the conclusion is drawn here that it is appropriate to compare these normalized results in this way. Between the 6 D and the 23 D locations the results evolve to reasonably approximate the Laufer results both qualitatively and quantitatively. The distributions along the Y axis exhibit a skewness that is undoubtedly due to the extreme skewness in the mean axial flow profile produced by the elbow.

The vertical component of the turbulent velocity shown in Figures 6 and 7 deviates markedly from the Laufer distributions for locations within about 15 D from the elbow exit. The distribution versus X shown in Figure 7 approximates the Laufer results at about the 20 D location. However, the distributions shown versus Y in Figure 8 evolve to only remotely resemble Laufer results beyond the 20 D location.

Single Elbow Results with CRV Installed

A summary of the LDV measurements made over about 25 D downstream of the single elbow with the CRV installed is given in Figures 9-16. These figures correspond to Figures 1-8 and duplicate nomenclature and the scales used above to display the results obtained without the CRV. Figures 1 and 2 and 9 and 10 indicate that the CRV produces flow conditions near the centerline of the pipe for measured locations between 2.7 and 12 D from the elbow exit for which the axial velocity component is within about 5% of the cross-sectional average velocity. However, it should also be noted that beyond the region near the center of this pipe the axial velocity deviations from the average can range to almost 20% at the half radius locations near the elbow exit. In this region, Figures 11 and 12 show the vertical component of the mean velocity ranges up to about ±8% of the average axial velocity.

Figures 13 and 14 indicate that the CRV seems to remove some of the features of the axial turbulence distributions shown in Figures 5 and 6 that qualitatively and quantitatively differ from the Laufer results. Similar conclusions can be drawn comparing Figures 15 and 16 with 7 and 8.

The comparisons of pipe flows exiting the single elbow for a Reynolds number of 10^5 without and with the CRV are shown for measurement locations within 12 D from the elbow in Figures 17-20. As before, nomenclature and results denoted by solid lines are the same. Figures 17 and 18 clearly show that the CRV produces axial velocity levels near the pipe centerline that are within 5% of the cross-sectional average value. In this same region the mean vertical or cross-flow component is within ±8% of the cross-sectional average value. Figures 19 and 20 show more clearly the conclusions drawn above that the CRV produces axial and vertical turbulent velocity distributions that more closely approximate Laufer results than those produced by the single elbow near its exit.

Closely-Coupled Double Elbows Out-of-Plane CRV Installed Configuration

A summary of the LDV measurements made over about 95 D downstream of the closely-coupled double elbows out-of-plane configuration is given in Figures 21-28, see Refrs. 1 and 5. As before, the time-averaged, axial velocity distributions denoted "Bogue and Metzner" are considered to be the reference distributions for fully developed pipe flow. The fully developed, turbulent velocity distributions are considered to be the distributions measured by Laufer.

Figures 21-24 show mean velocity components in the axial and vertical directions plotted versus the X and Y axes, respectively. For the axial velocity component, results deviate from the Bogue and Metzner distribution by as much as 25% as measured 2.6 D downstream of the exit of the second elbow to as little as about 5% at the Z = 95 D location. Vertical components of mean velocity also deviate by about 25% from ideal at the 2.6 D location to about 5% at the 95 D location.

Figures 25-28 show rms components of the turbulent velocity in the axial and vertical directions plotted versus the X and Y axes, respectively. The characteristic feature of these results are that the axial and vertical components deviate qualitatively and quantitatively from the Laufer distributions at locations within about 12 D of the exit plane of this configuration.

However, beyond these locations, the results evolve, if only slowly, to reasonably approximate the Laufer distributions with further distance downstream, until the 95 D station where they exhibit close agreement with Laufer's results. It is noted from Figure 28 that the vertical turbulence velocity component along the Y axis shows distributions that are markedly different from Laufer's results for the locations measured, but these exhibit consistencies at the pipe centerline with the distributions shown in Figure 27.

Closely-Coupled, Double Elbows Out-of-Plane Configuration with CRV Installed

A summary of the LDV measurements made over about 30 D downstream of the closely-coupled double elbows out-of-plane configuration with the CRV installed as shown in Sketch 3 is given in Figures 29-36. These figures use the pipe coordinate system shown in Sketch 3 which also gives the relationships between the pipe coordinate system and the laboratory system used previously. Figures 29 and 30 indicate that, near the exit of this piping configuration, the CRV produces mean axial velocity distributions in the center core of this pipe flow that approximate the cross-sectional average velocity. Specifically, within a center core region of about 10% of the pipe radius and between 2.6 and 6 D from the exit, the axial velocity of this conditioned pipe flow is within 5% of the cross-sectional average velocity. Figures 31 and 32 show the effects of the CRV on the strong and slowly decaying swirl that is plotted in Figures 23 and 24. The CRV changes significantly the axial component of the velocity measured immediately downstream of the exit of this pipe flow. The CRV appears to both reduce and confine this clockwise (looking upstream) swirl to the region near the pipe centerline, and it achieves this result through its imposing counter-clockwise flow rotation on this flow that is shown in Figure 31 for all locations measured. This swirl imposition is noted to be very strong near the pipe wall at the upstream locations and it diffuses radically inward to the pipe centerline with downstream distance. At the 30 D station the CRV conditioned pipe flow shows only small levels of solid-body, counter-clockwise swirl. Comparing Figures 24 and 32 shows further that the CRV has a strong effect on the pipe flow near the exit of this configuration. Near the pipe centerline, the initially low level of mean vertical velocity now is shown to have large and negative V_p components. These effects are undoubtedly related to the radial shifts found in the swirl distributions in Figure 31.

Figures 33-36 show the CRV effects on the rms distributions of the axial and vertical components of the turbulent velocity. Comparing Figures 25 and 33 and 26 and 34 indicates that within about 6 D of the exit of this pipe configuration; the CRV does not seem to change the cross-sectional average value of the axial component of the turbulent velocity. However, these comparisons do indicate that the CRV redistributes the turbulence. Comparing Figures 27 and 35 and 28 and 36 reaffirms this observation for the vertical component of the turbulent velocity between 2.7 and 6 D of the exit of this configuration.

Figures 37-39 directly compare corresponding measurements of the pipe flows from the closely-coupled double elbows out of plane configuration with and without the CRV. The mean axial velocity component plotted versus radial pipe coordinates is shown in Figures 37 and 38. As noted above, within a core region near the pipe centerline and near the exit of this configuration, the CRV conditioned flows have velocity levels within 5% of the cross-sectional average. These results also show that for downstream distances beyond the 5 D distance to about the 10 D location, the mean axial velocities in the center core region closely approximate the average. These figures also indicate clearly the significant changes in the mean axial velocity distributions produced by the CRV. In a similar way, these results show the CRV effects on the rms distributions of the axial component of the turbulent velocity produced by the CRV and the deviations these have from Laufer's results.

Figure 39 shows radial component distributions for both the mean and rms components of the radical velocities with and without the CRV. Comparisons of the mean components are more directly noted for the corresponding measurements and clearly show the significant conditioning effects produced by the CRV. These indicate that the CRV generates radial components of approximately 10% of the cross-sectional average velocity near the pipe centerline and very near the exit of this configuration at 2.70. Between 6 D and 12 D, the vertical mean velocity component in the CRV conditioned flows is noted to be less than 8% of the cross-sectional average.

Conclusions

The results of these special tests on the effects of the CRV in the selected piping configurations for these fluid and flow conditions indicate that it can produce regions in these pipe flows where appropriate measurement techniques can achieve accuracy levels at, or better than 5%. These results are due to the fact that the CRV-conditioned flows have a localized region in a center core region about the pipe centerline where the mean axial velocity component is within 5% of the cross-sectional average velocity. This region is near the pipe center line and near the exit plane of these two piping configurations. Specifically, near the pipe centerline means within about 5% of the pipe radius and near the single elbow exit means between 2.7 and 12 D downstream. For the closely-coupled, double elbow configuration near the exit means between 2.6 and 12 D downstream. Results also show that stations nearer the exit and further than these locations may have mean axial velocities that deviate further than 5% from the cross-sectional average. Therefore, the center of this region, i.e., on the pipe centerline at about 9 D downstream from the exit is concluded to be the location where highest flow measurement accuracies can be obtained.

To use this localized region to make improved accuracy flow measurements, it is important to select an appropriate technique. This technique should be one that can determine high levels of spatial resolution. It should be insensitive to other components of the mean velocity and it should not be disturbed by such turbulence levels as occur in these localized regions.

If such a strategy as described above is used to make accurate flow measurements in these flow conditioned situations, it is recommended to calibrate the technique and the instrument in the specific fluid and flow situation to assess and quantify performance. When such calibration facilities are realistically traceable to appropriate standards, the levels of success of the strategy can be quantified and assured, accordingly.

References

1. Mattingly, G.E. and Yeh, T.T., Effects of Pipe Elbows and Tube Bundles on Selected Types of Flowmeters, Flow Measurement and Instrumentation Journal, 1991, Vol. 2 pp 1-19.

2. Mattingly, G.E. and Yeh, T.T., NIST's Industry-Government Consortium Research Program on Flow Meter Installation Effects: The Single Elbow, NISTIR 89-4080, April 1989, NIST, Gaithersburg, MD.

3. Bogue, D.C. and Metzner, A.B., Velocity Profiles in Turbulent Pipe Flow, I&EC Fundamentals 2, (2), 1963 pp. 143-149.

4. Laufer, J., The Structure of Turbulence in Fully Developed Pipe Flow, NBS Report 1974, Sept. 1952.

5. Mattingly, G.E. and Yeh, T.T., NIST's Industry-Government Consortium Research Program on Flow Meter Installation Effects: The Closely-Coupled Elbows Out-of-Plane Configuration, NISTIR 88-3898, May 1988.

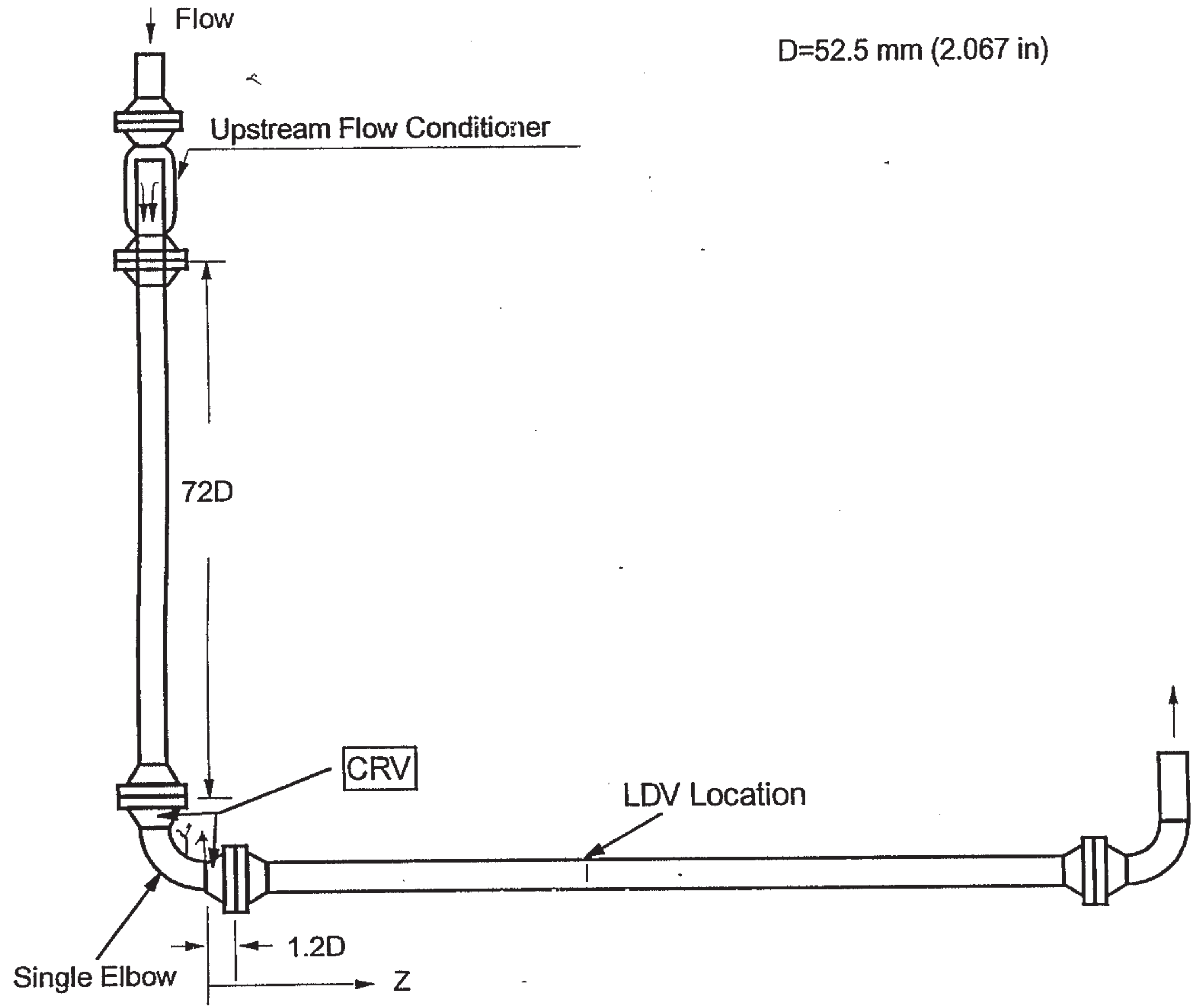

Sketch 1 Single Elbow Piping Configuration. (The coordinate system used is a right-handed system with Z as shown. The X coordinate is into the page, and Y is upward. The origin of the coordinate system is the centerline of the pipe in the exit plane of the elbow.)

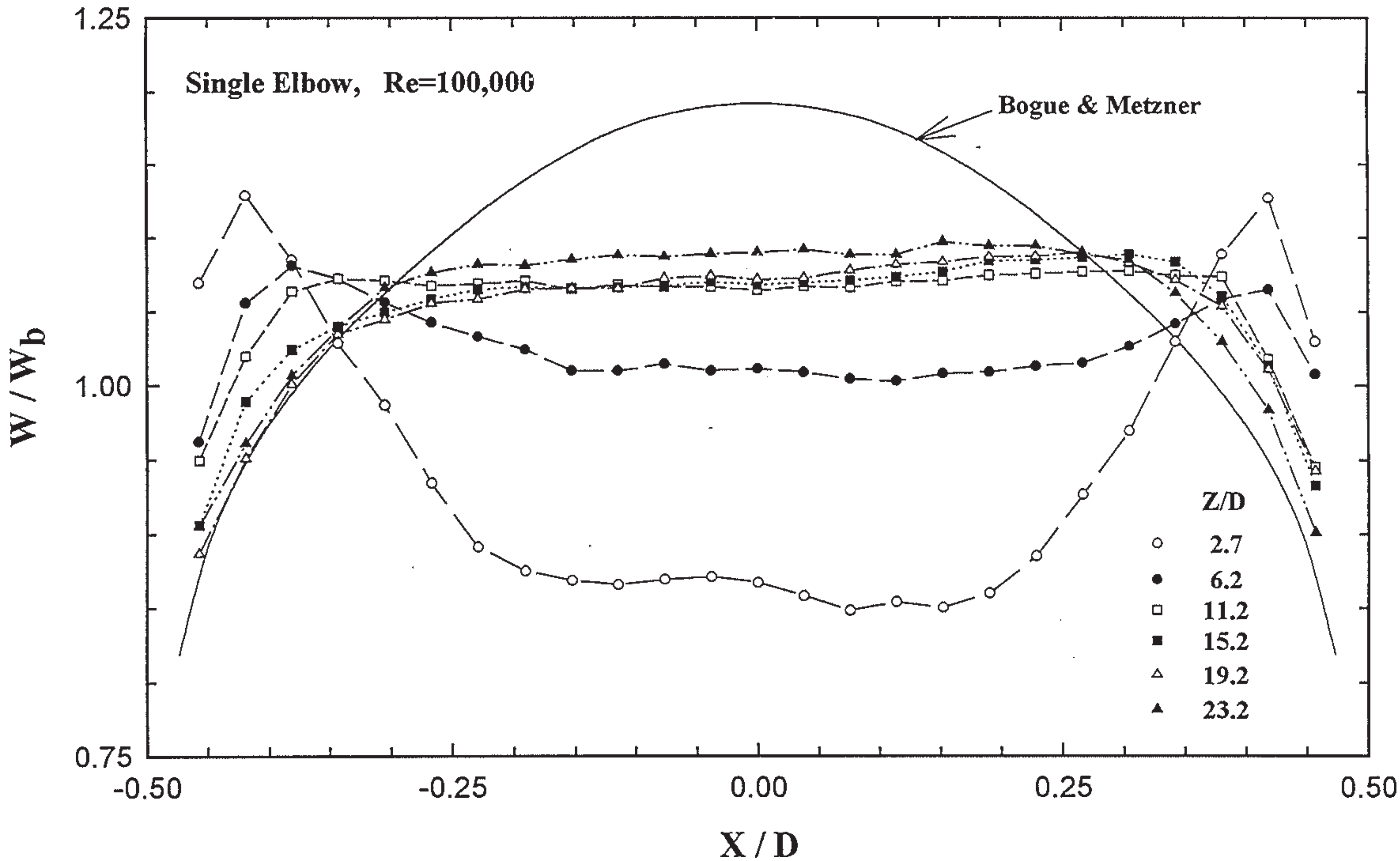

Figure 1 **Profiles of the Axial Mean Velocity vs. Horizontal Radial Position at Different Downstream Locations.**

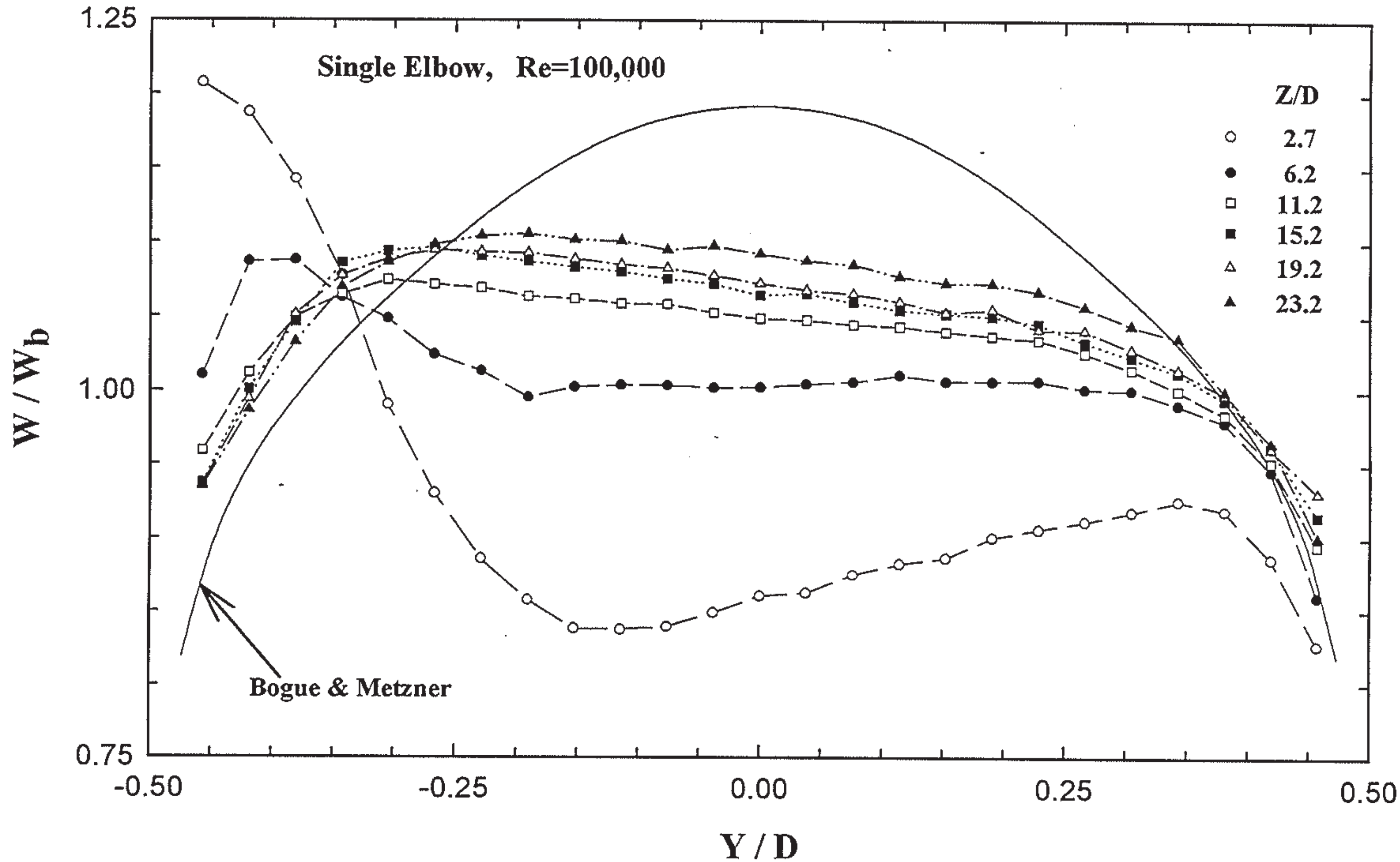

Figure 2 **Profiles of the Axial Mean Velocity vs. Vertical Radial Position at Different Downstream Locations.**

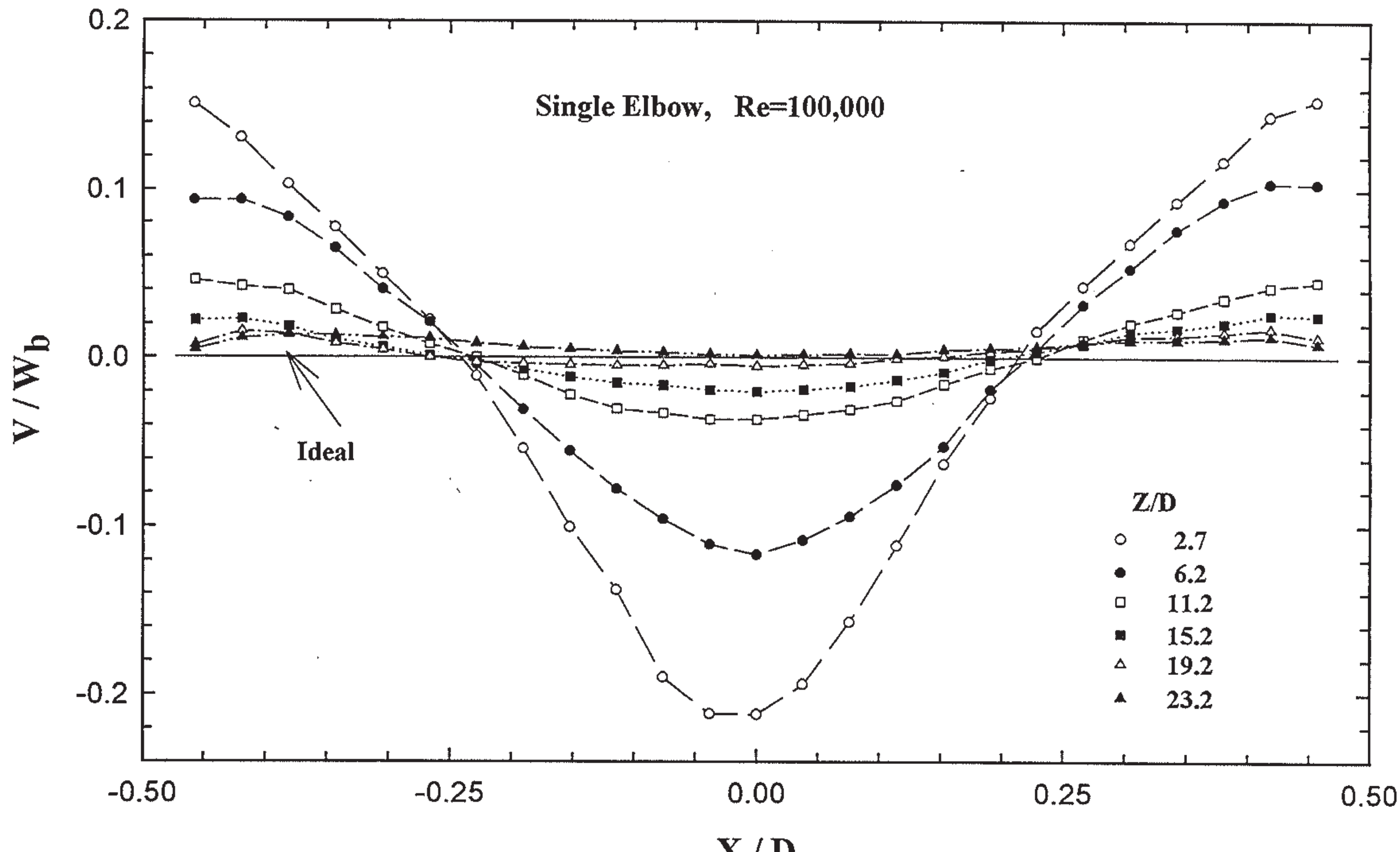

Figure 3 Profiles of the Vertical Mean Velocity vs. Horizontal Radial Position at Different Downstream Locations.

V5MY

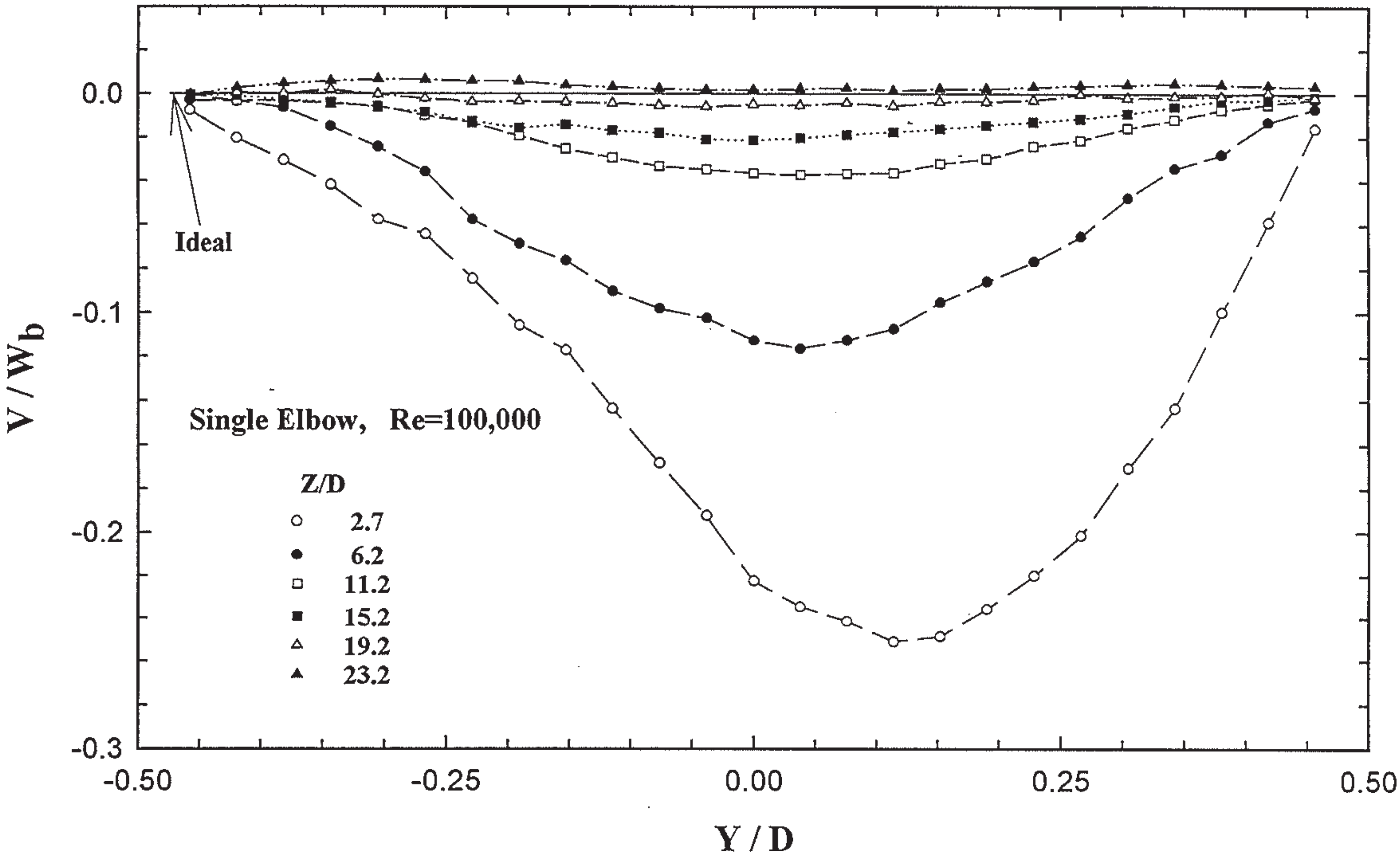

Figure 4 Profiles of the Vertical Mean Velocity vs. Vertical Radial Position at Different Downstream Locations.

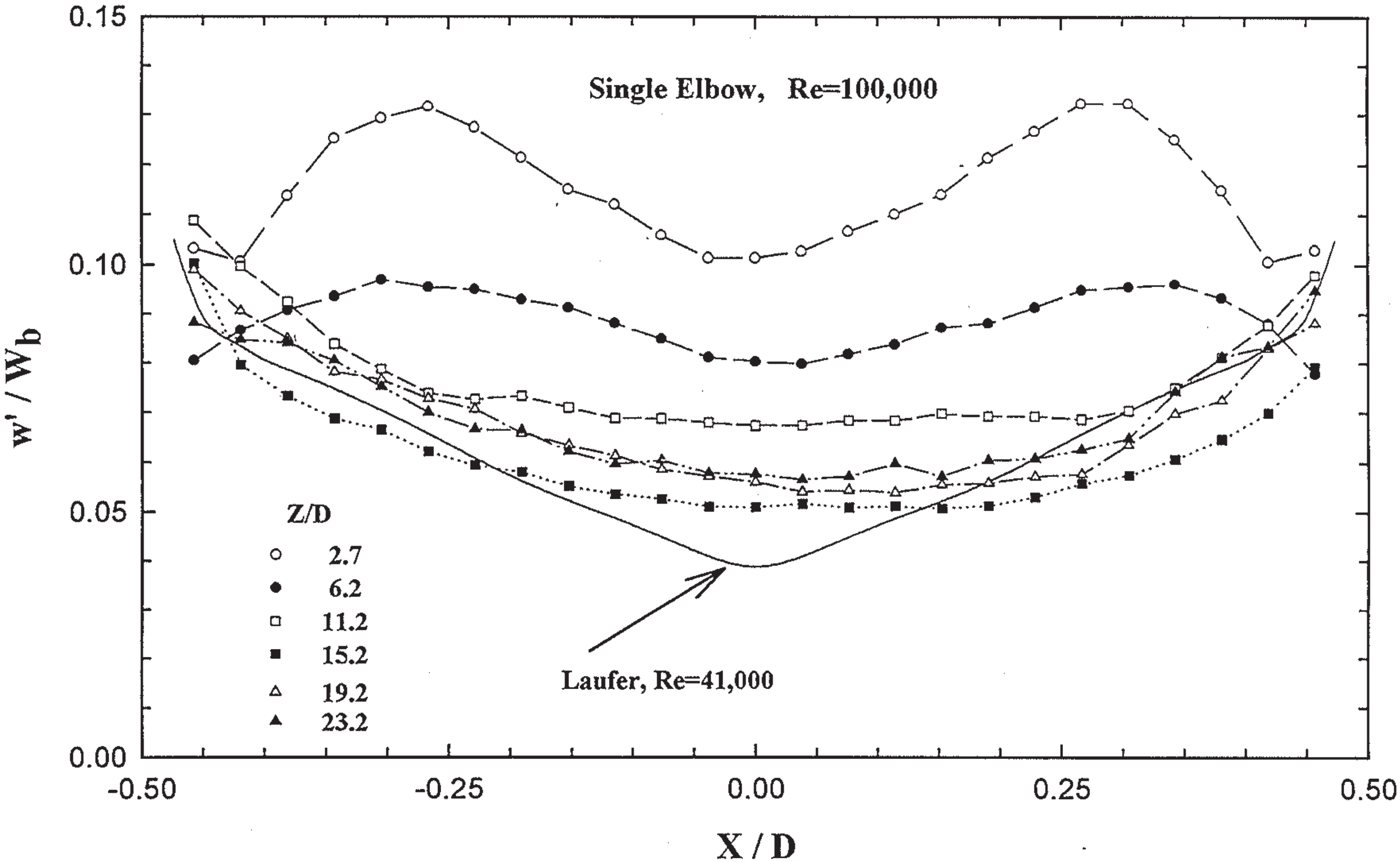

Figure 5 Profiles of the Axial Turbulent Velocity vs. Horizontal Radial Position at Different Downstream Locations.

W5TY

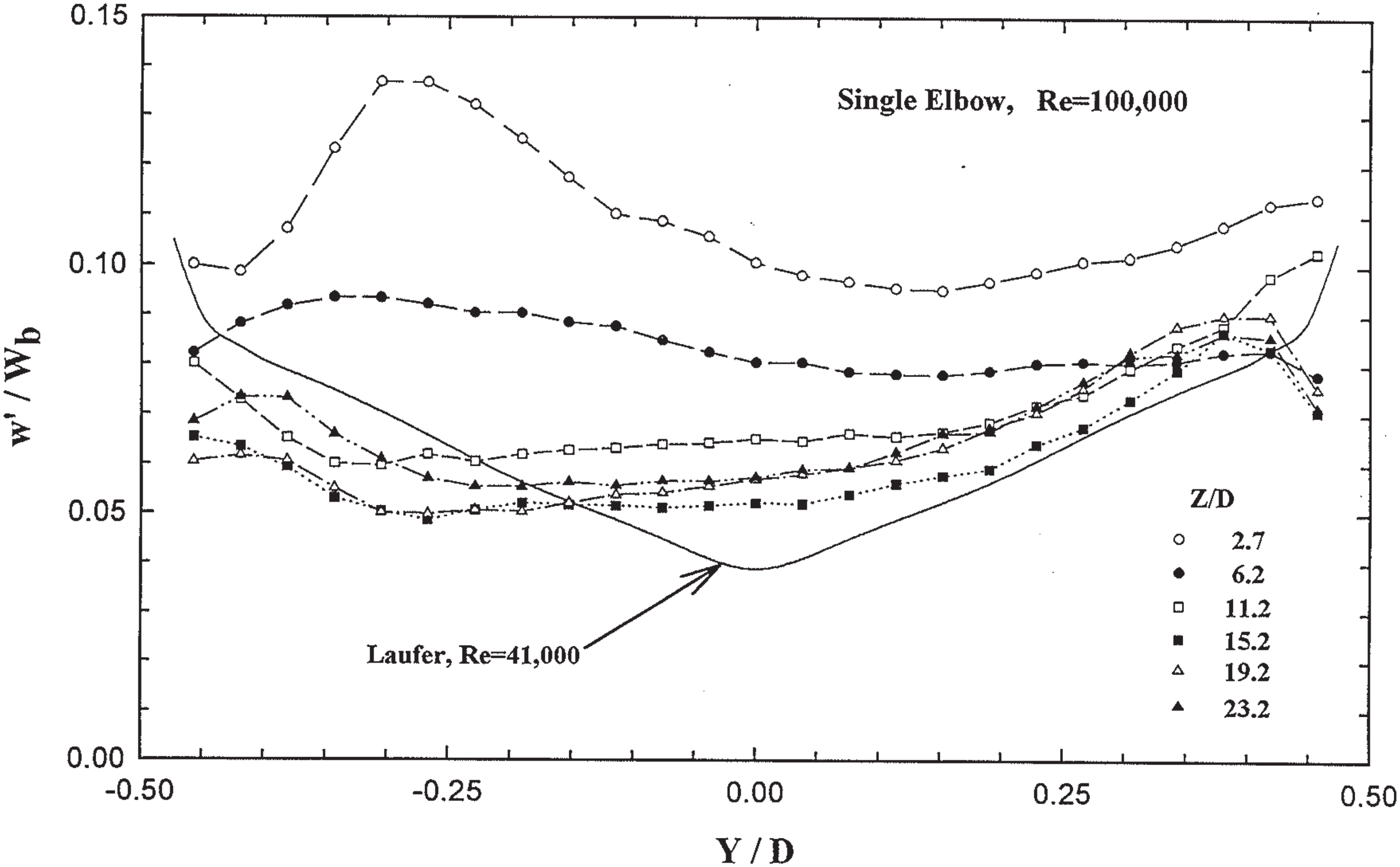

<u>Figure 6</u> Profiles of the Axial Turbulent Velocity vs. Vertical Radial Position at Different Downstream Locations.

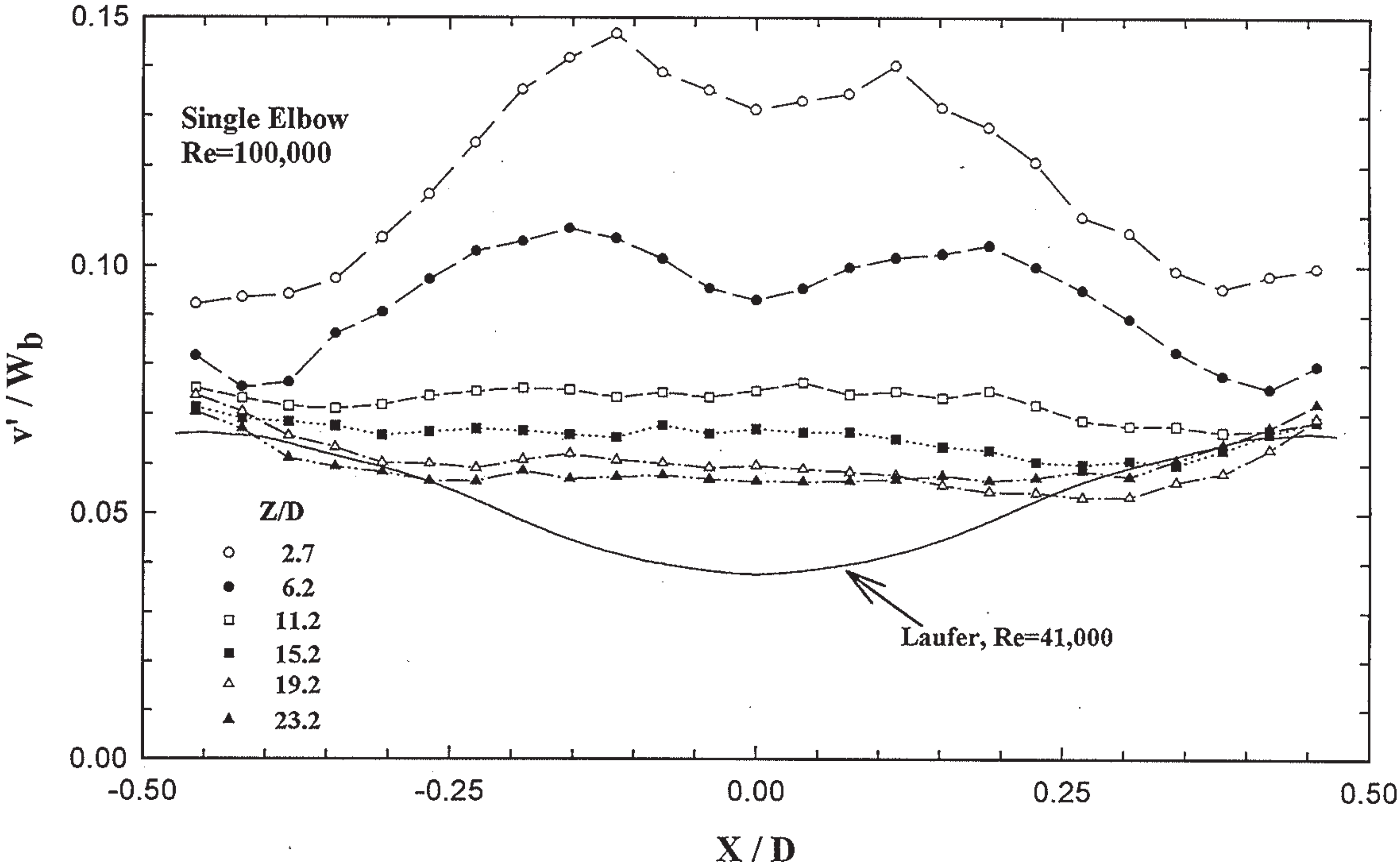

Figure 7 **Profiles of the Vertical Turbulent Velocity vs. Horizontal Radial Position at Different Downstream Locations.**

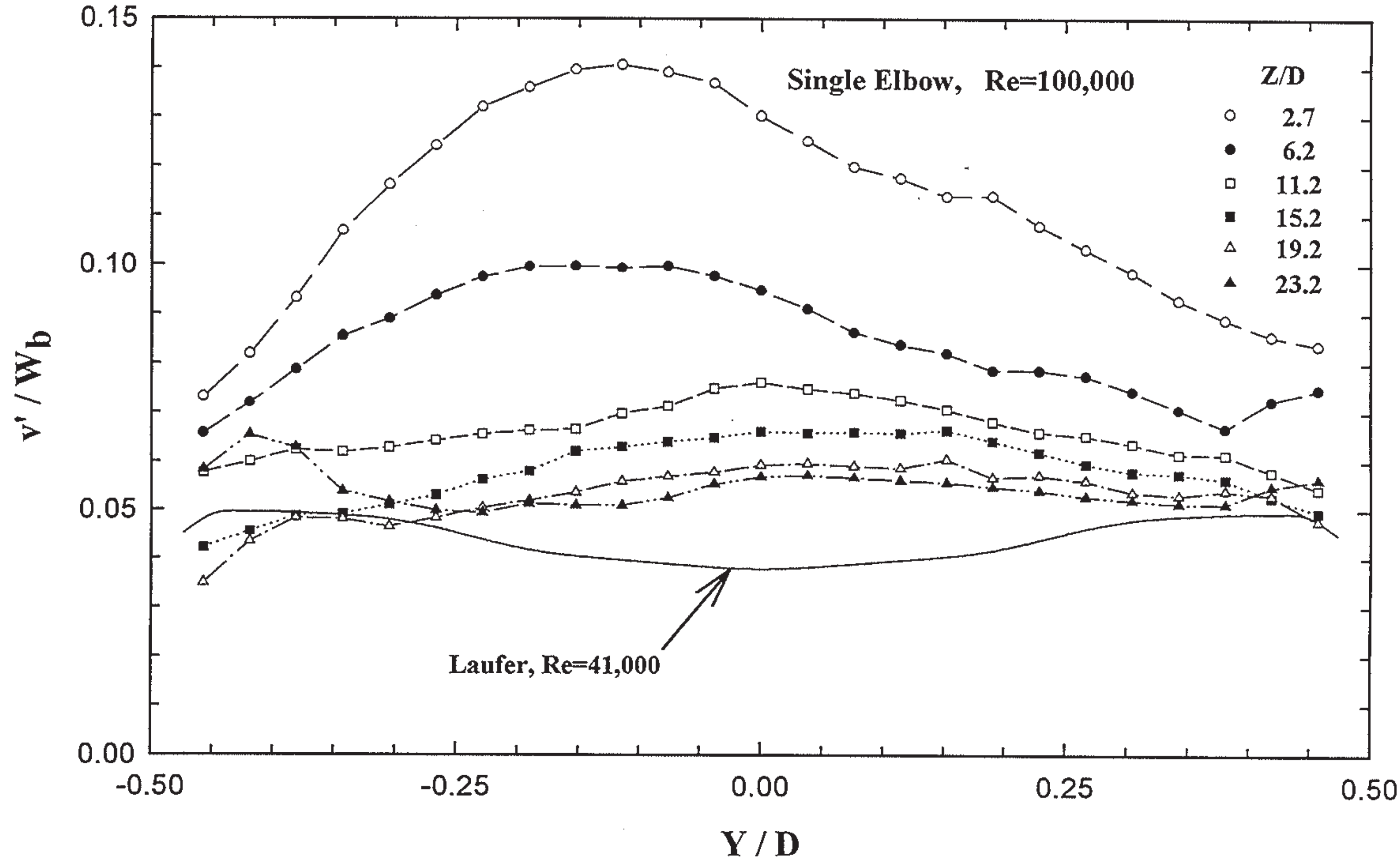

Figure 8 Profiles of the Vertical Turbulent Velocity vs. Vertical Radial Position at Different Downstream Locations.

WMX

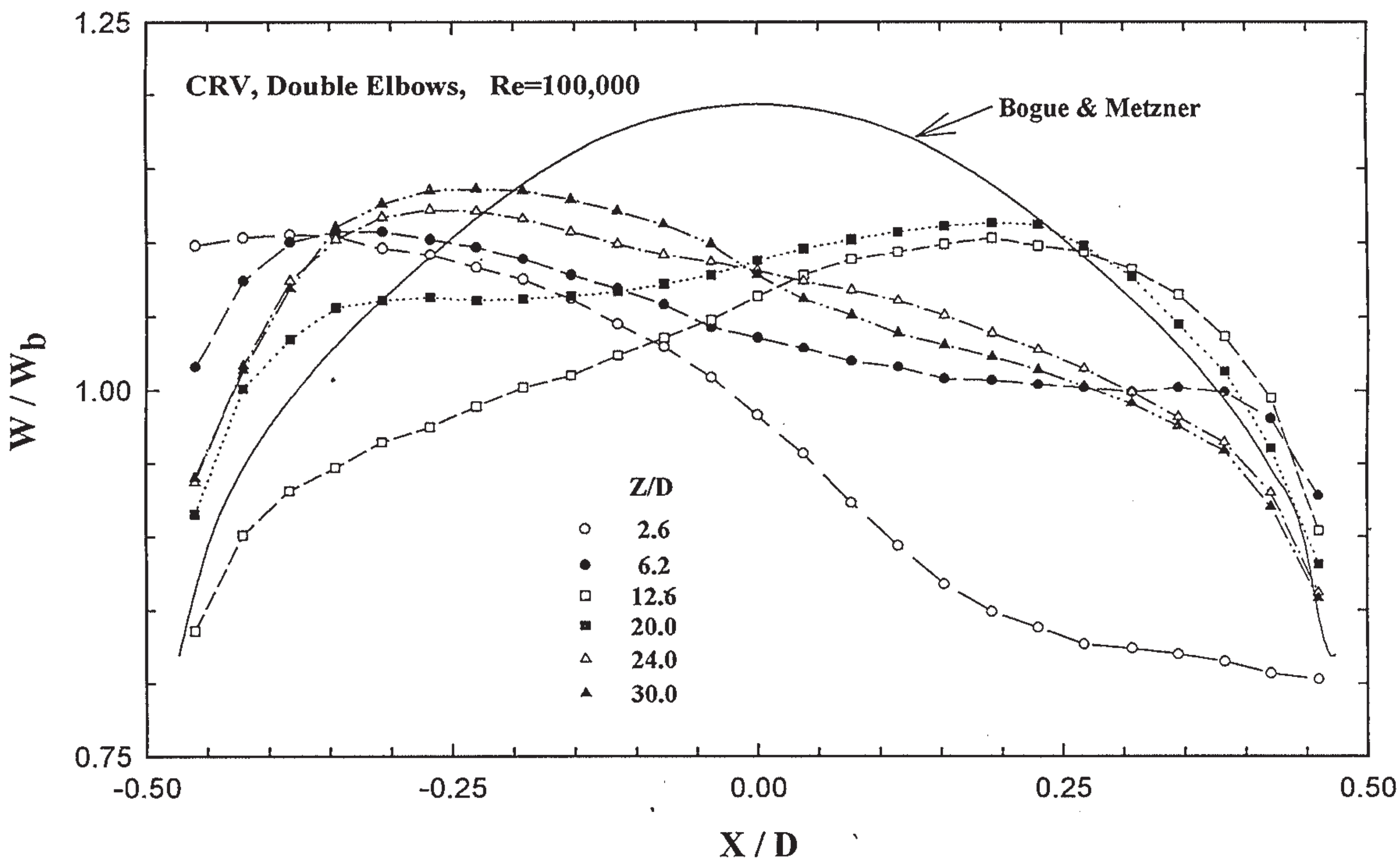

Figure 9 **Profiles of the Axial Mean Velocity vs. Horizontal Radial Position at Different Downstream Locations.**

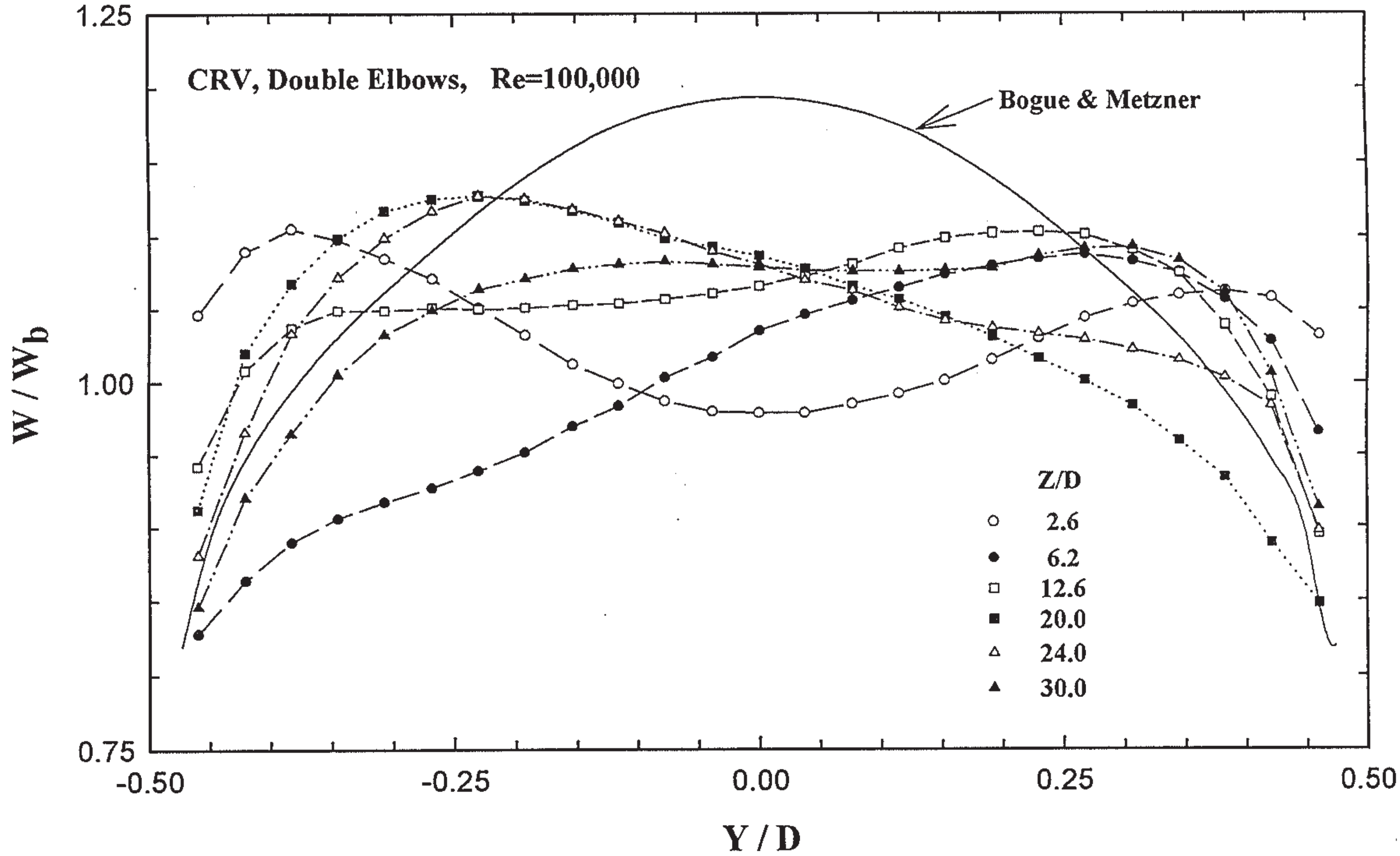

Figure 10 Profiles of the Axial Mean Velocity vs. Vertical Radial Position at Different Downstream Locations.

VMX

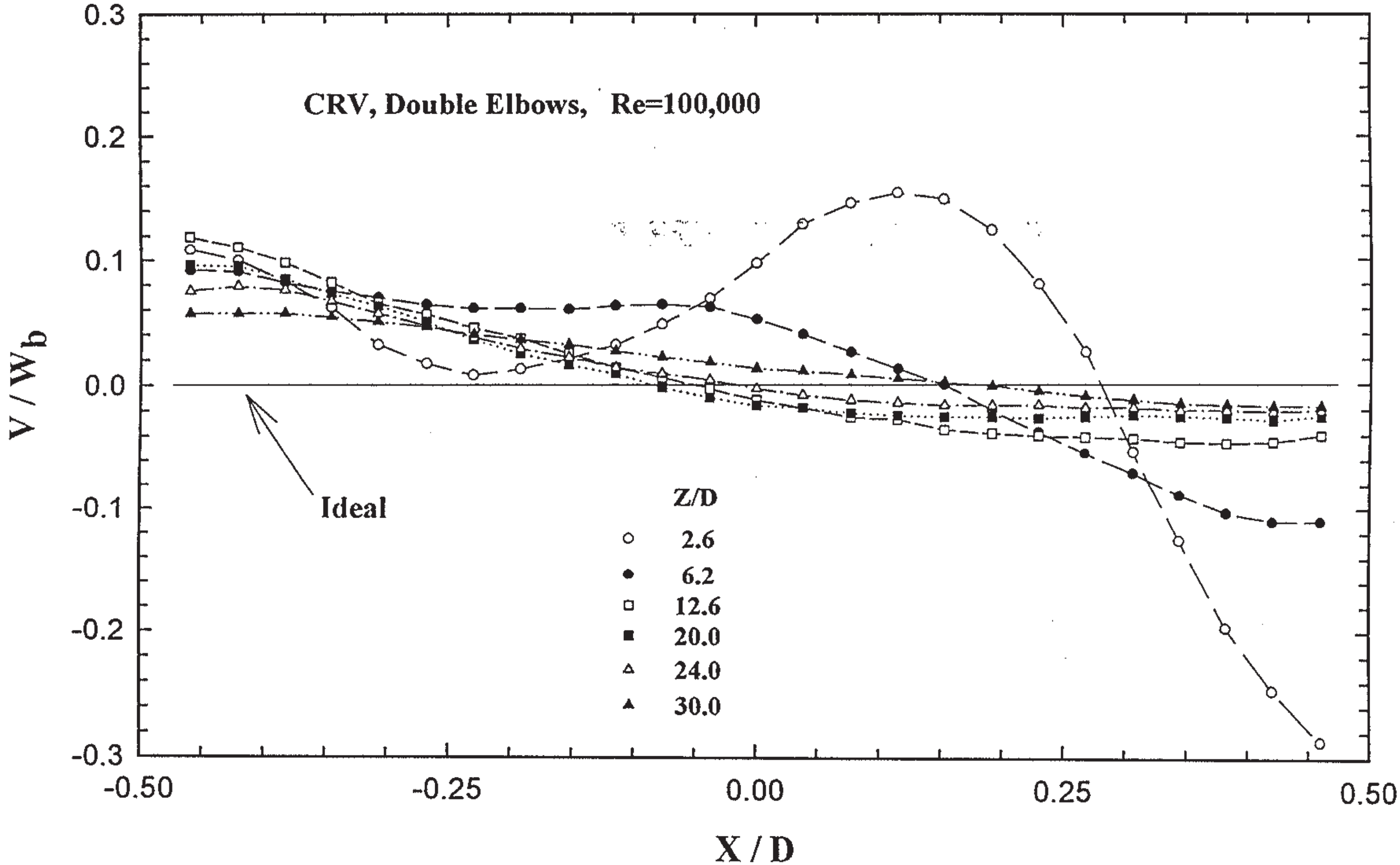

Figure 11a Profiles of the Vertical Mean Velocity vs. Horizontal Radial Position at Different Downstream Locations.

VMX

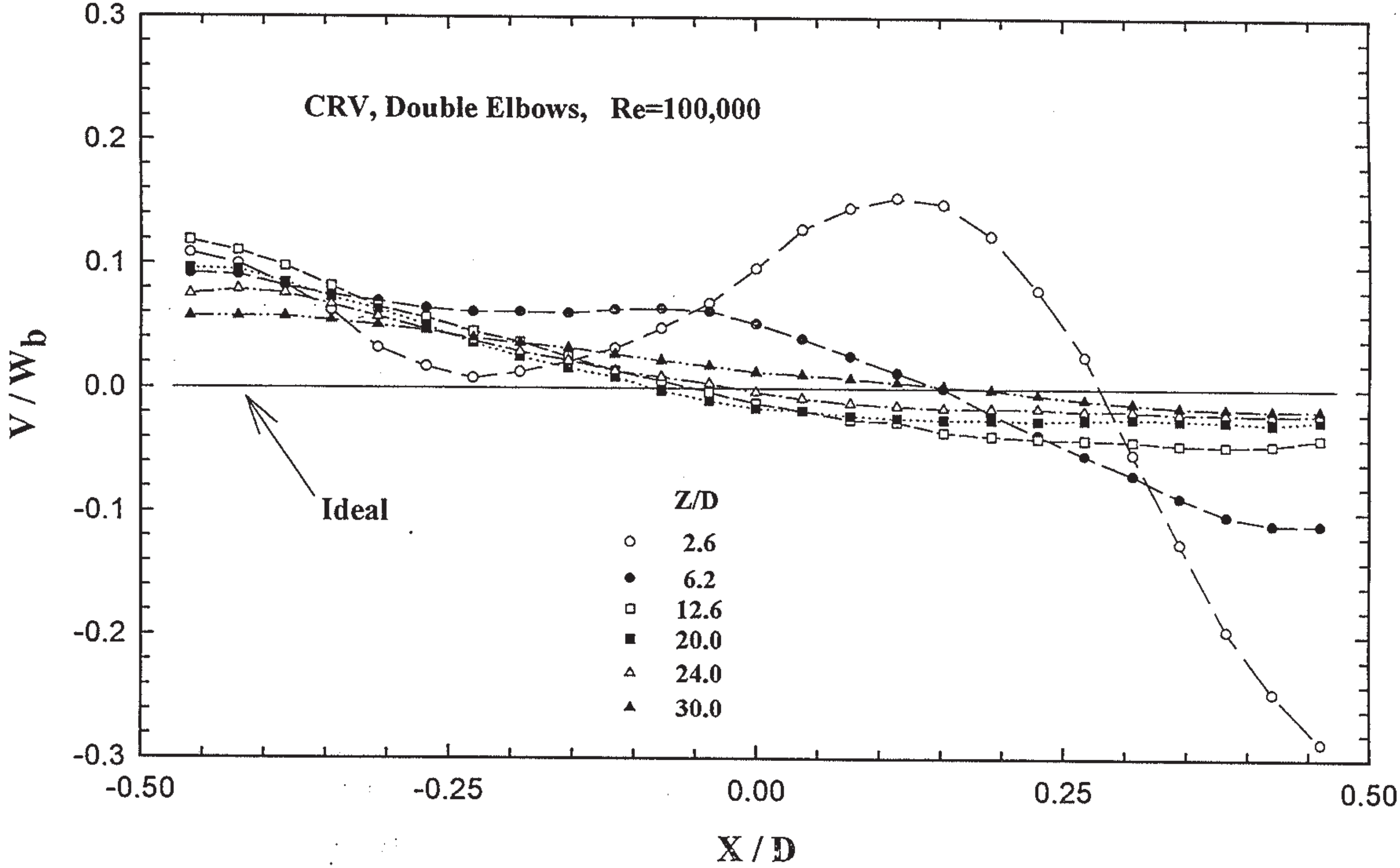

Figure 11b Profiles of the Vertical Mean Velocity vs. Horizontal Radial Position at Different Downstream Locations.

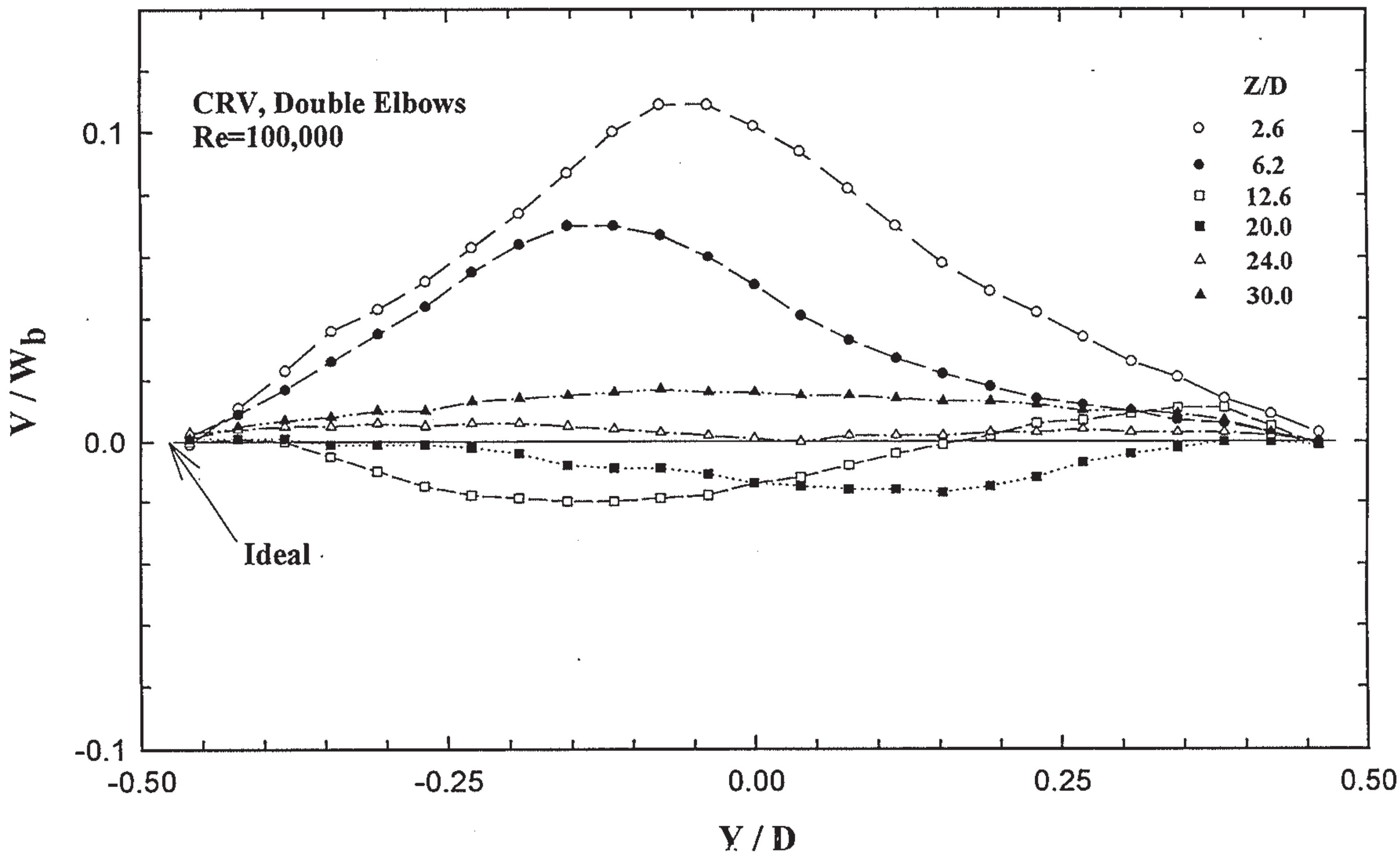

Figure 12a Profiles of the Vertical Mean Velocity vs. Vertical Radial Position at Different Downstream Locations.

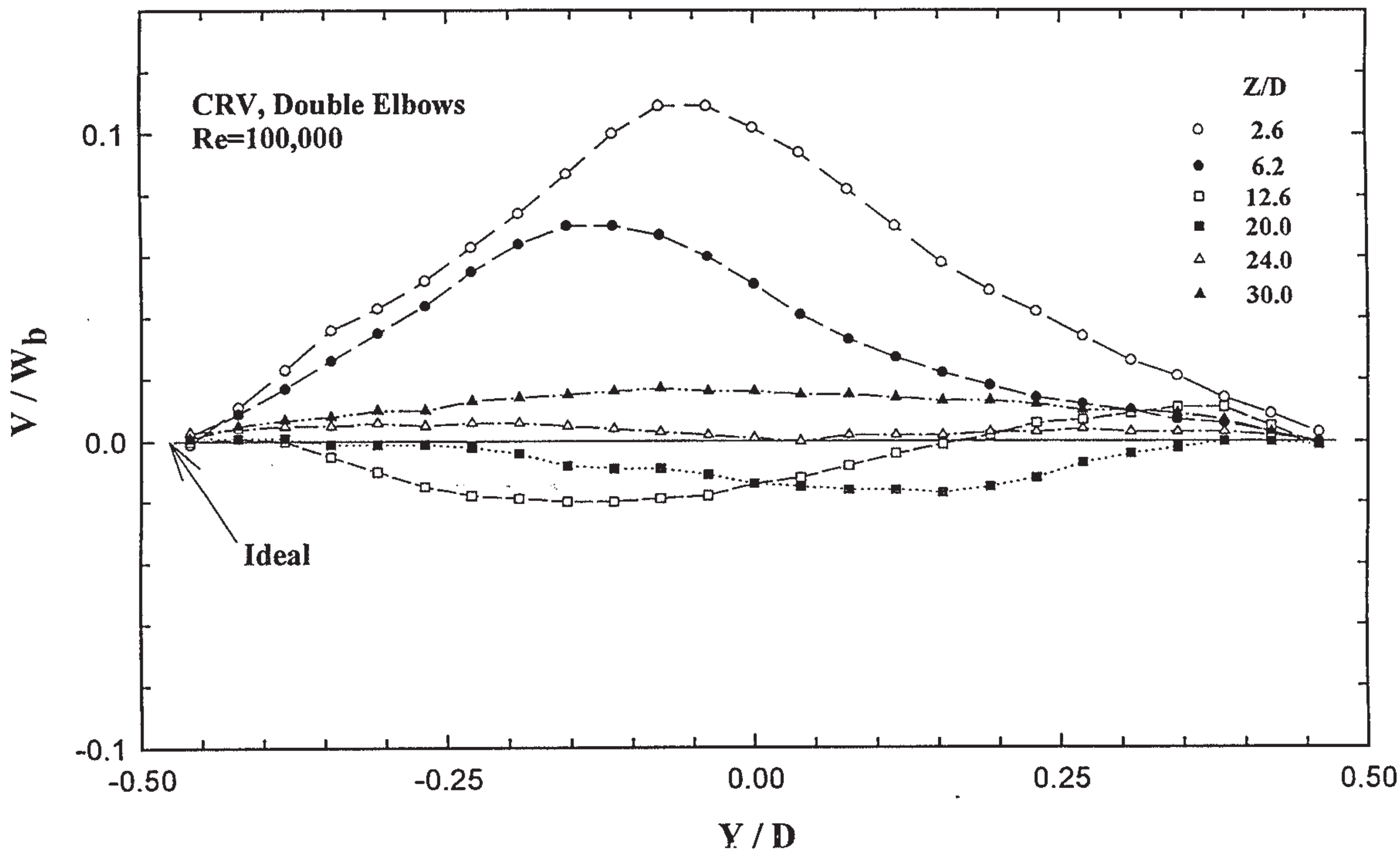

Figure 12b Profiles of the Vertical Mean Velocity vs. Vertical Radial Position at Different Downstream Locations.

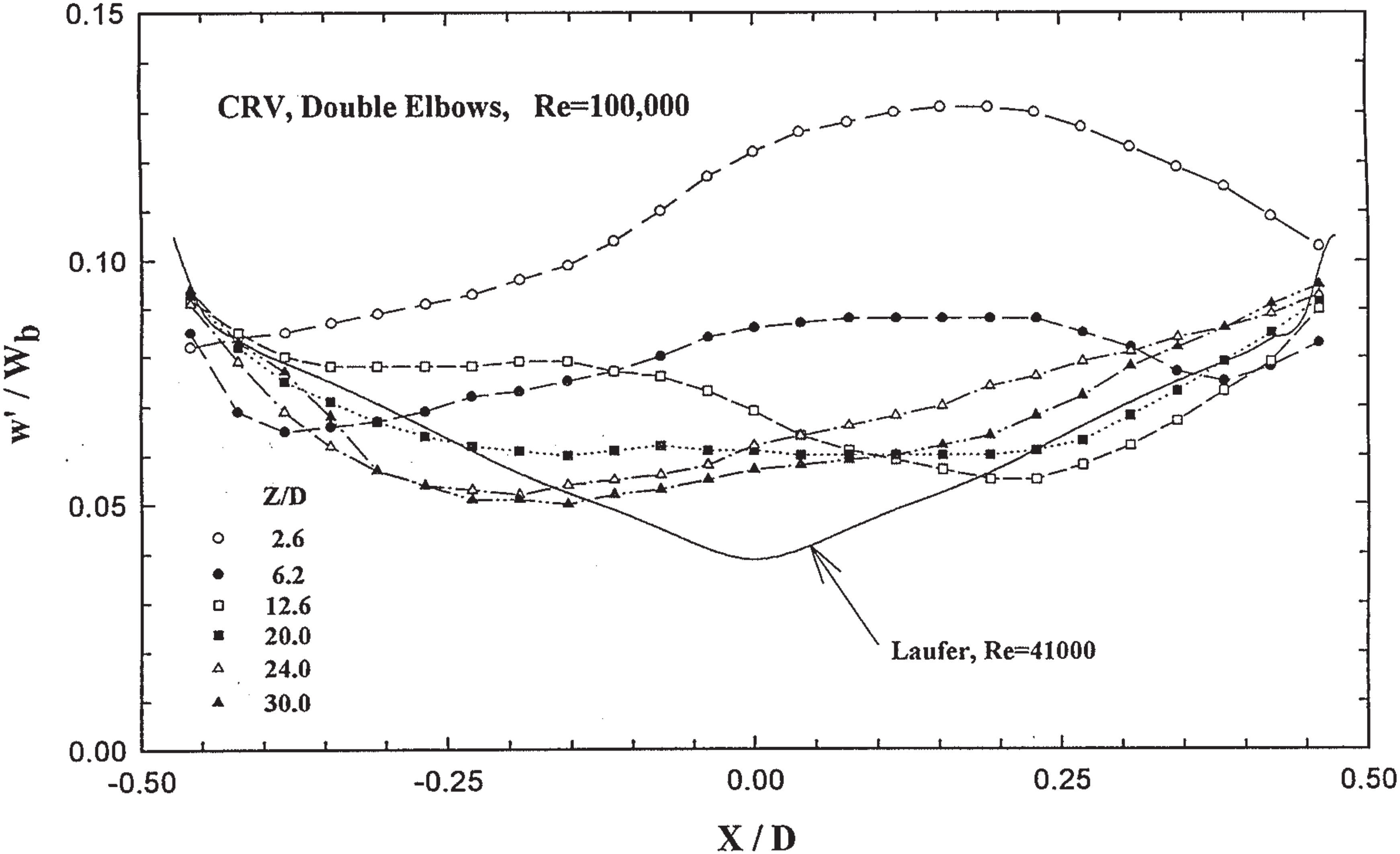

Figure 13 Profiles of the Axial Turbulent Velocity vs. Horizontal Radial Position at Different Downstream Locations.

WTY

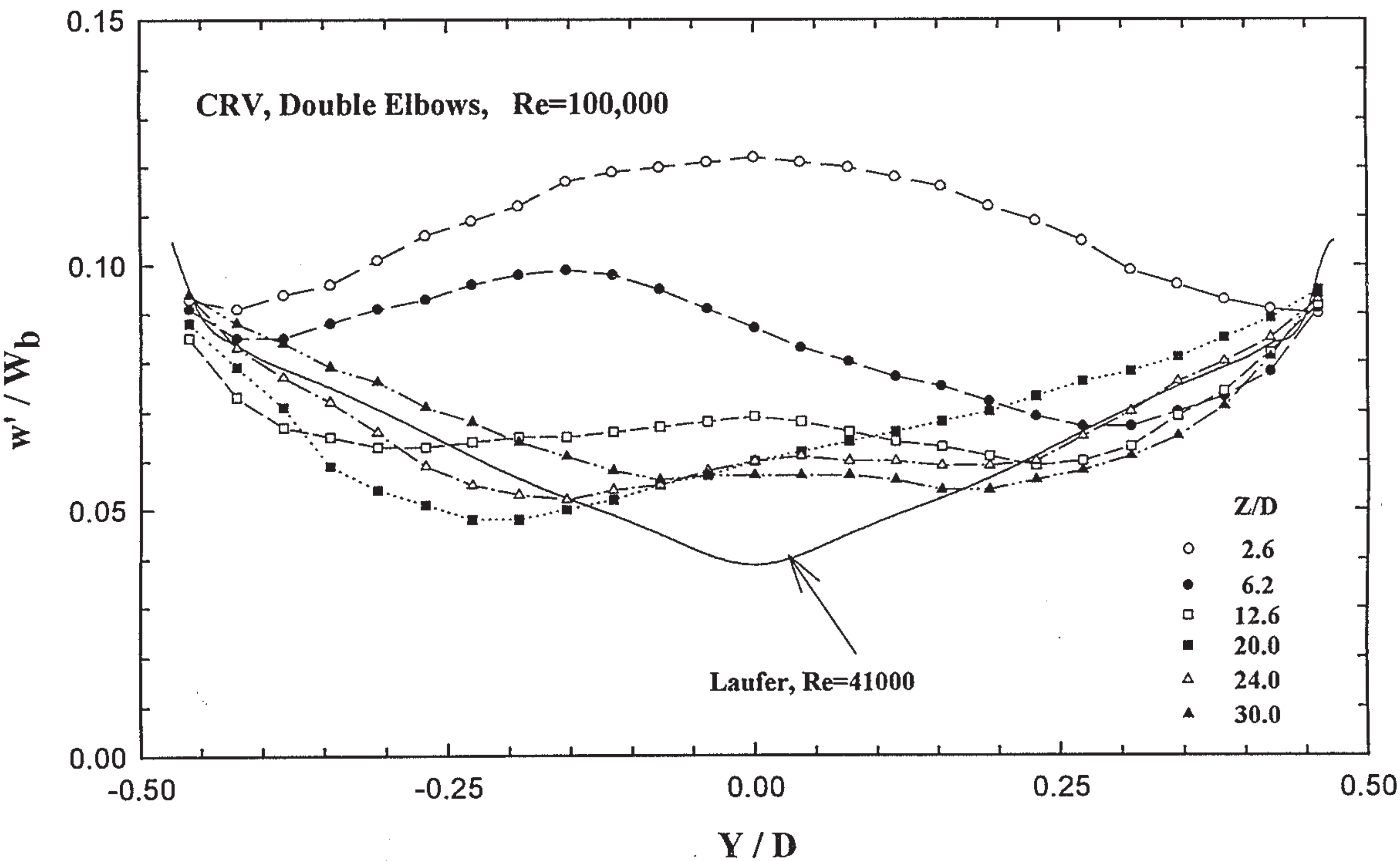

Figure 14 Profiles of the Axial Turbulent Velocity vs. Vertical Radial Position at Different Downstream Locations.

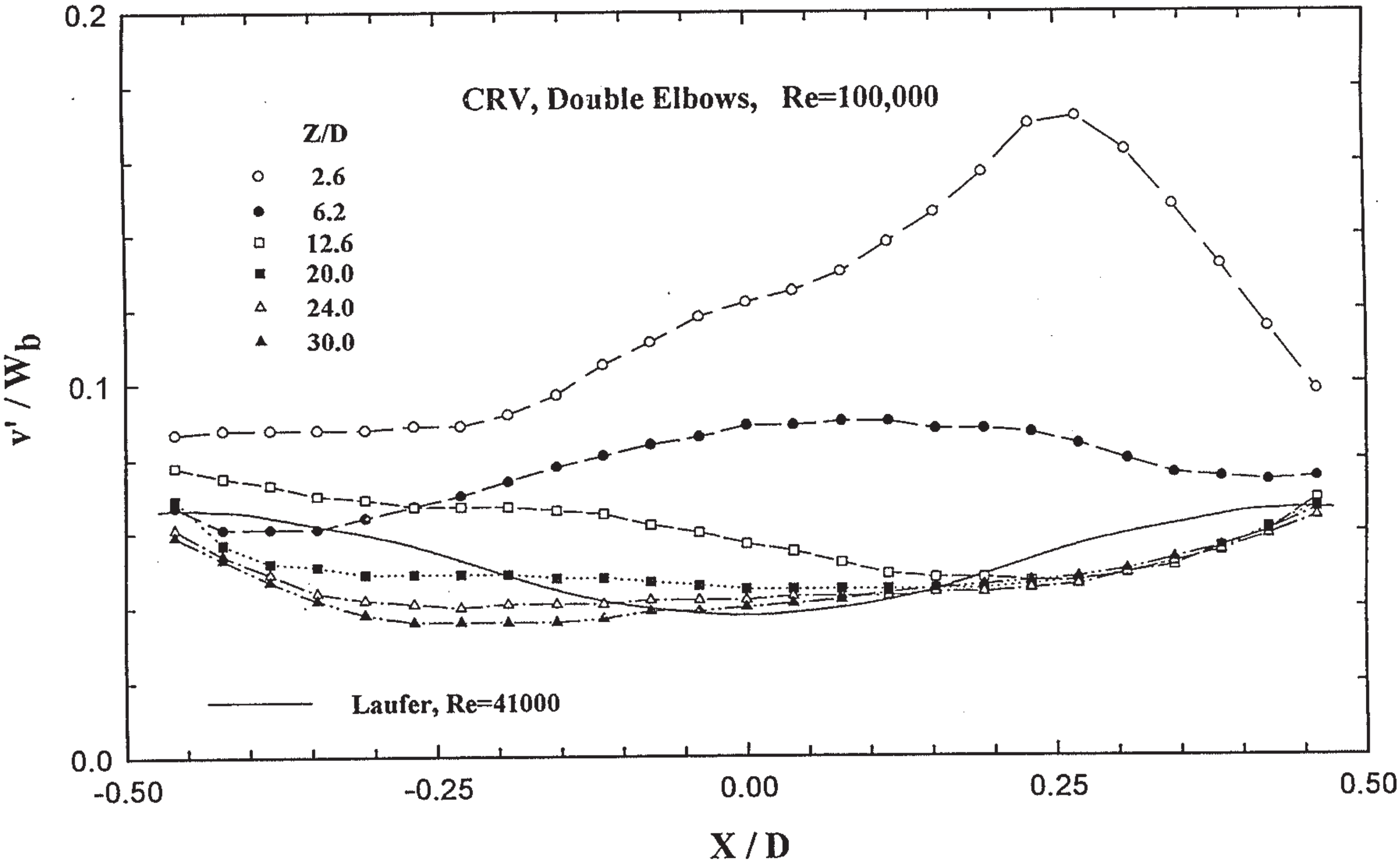

Figure 15 Profiles of the Vertical Turbulent Velocity vs. Horizontal Radial Position at Different Downstream Locations.

VTY

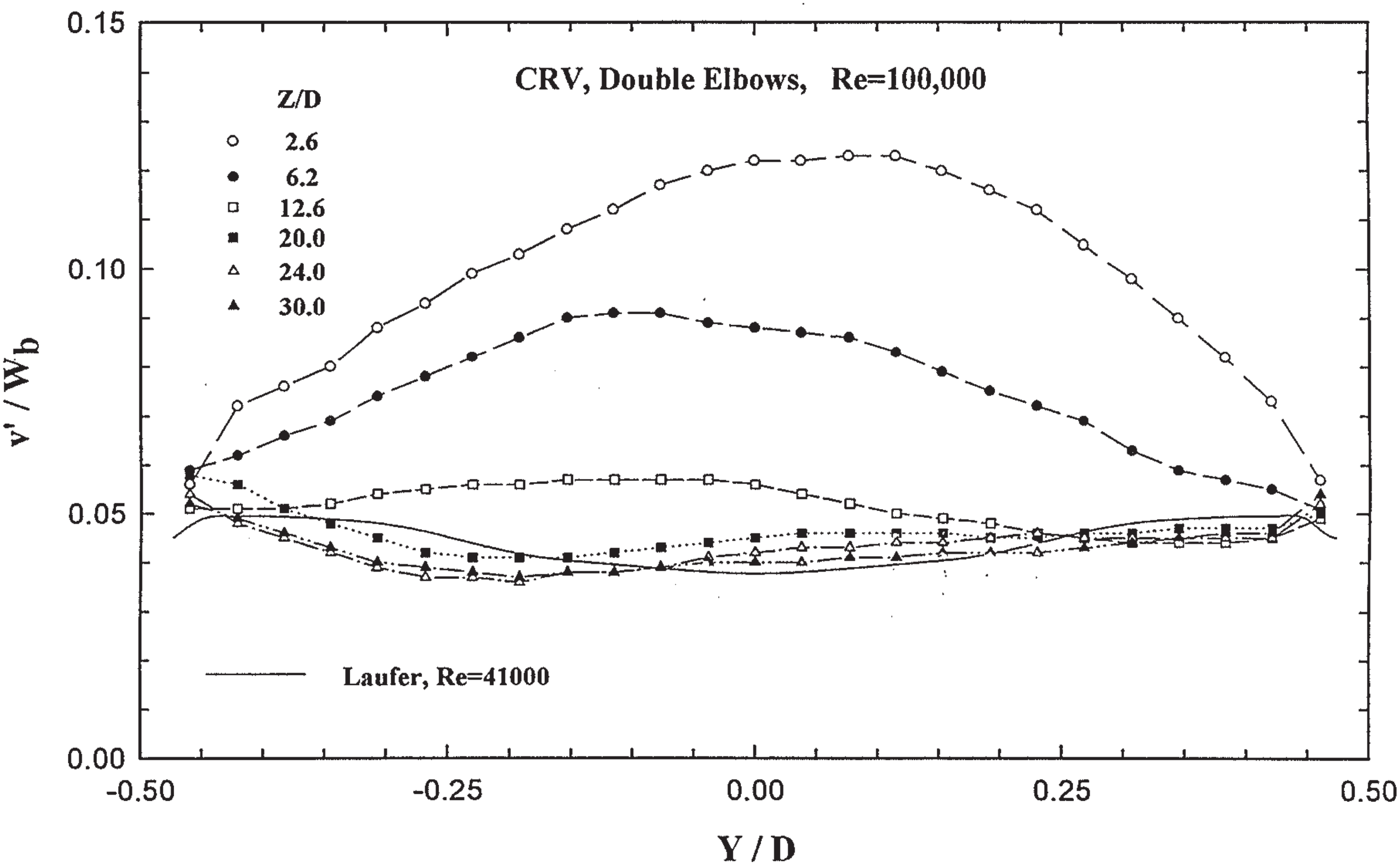

Figure 16 Profiles of the Vertical Turbulent Velocity vs. Vertical Radial Position at Different Downstream Locations.

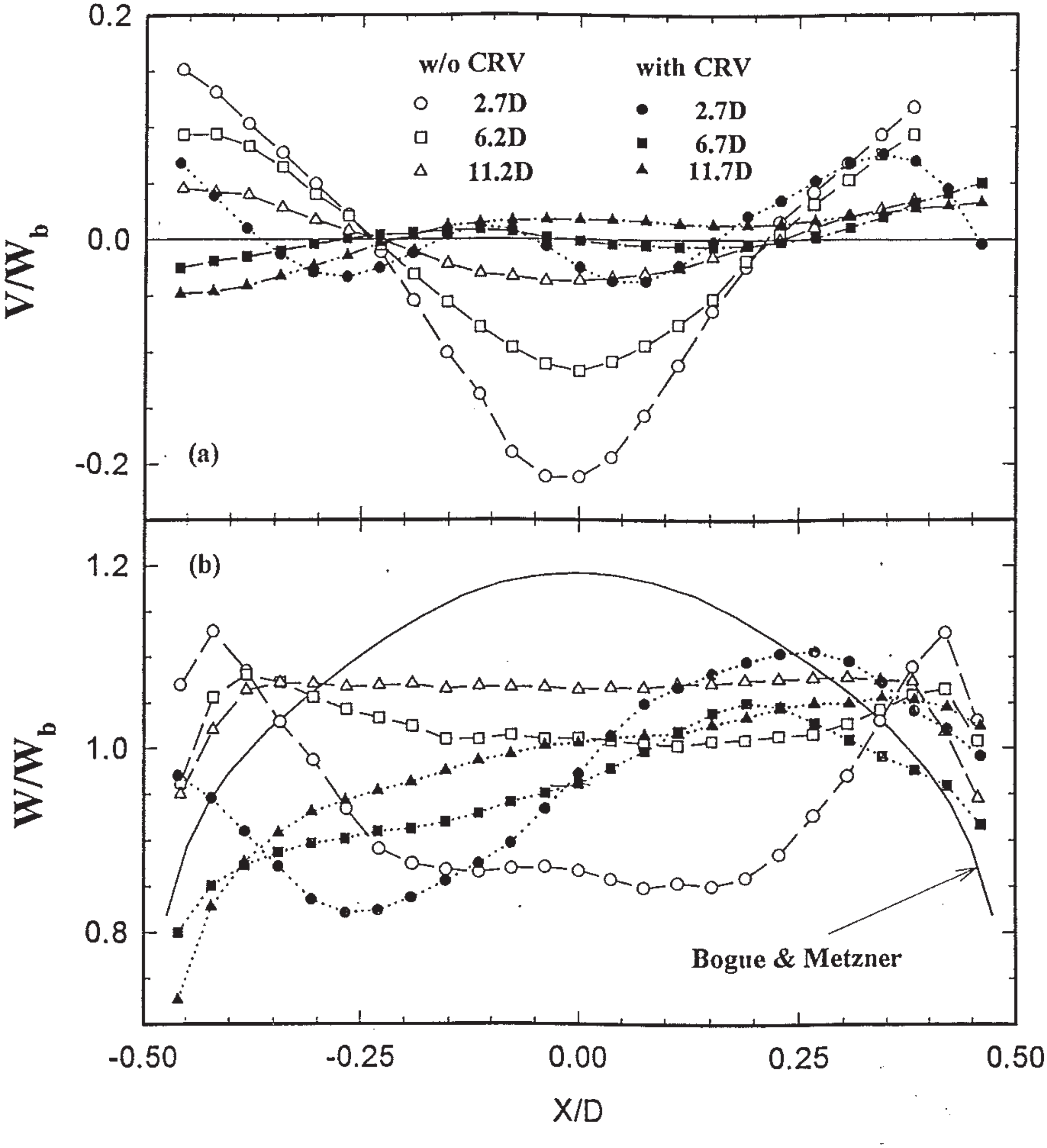

Figure 17 Comparison of Mean Velocity Profiles for Single Elbow with and without CRV for $Re=10^5$.

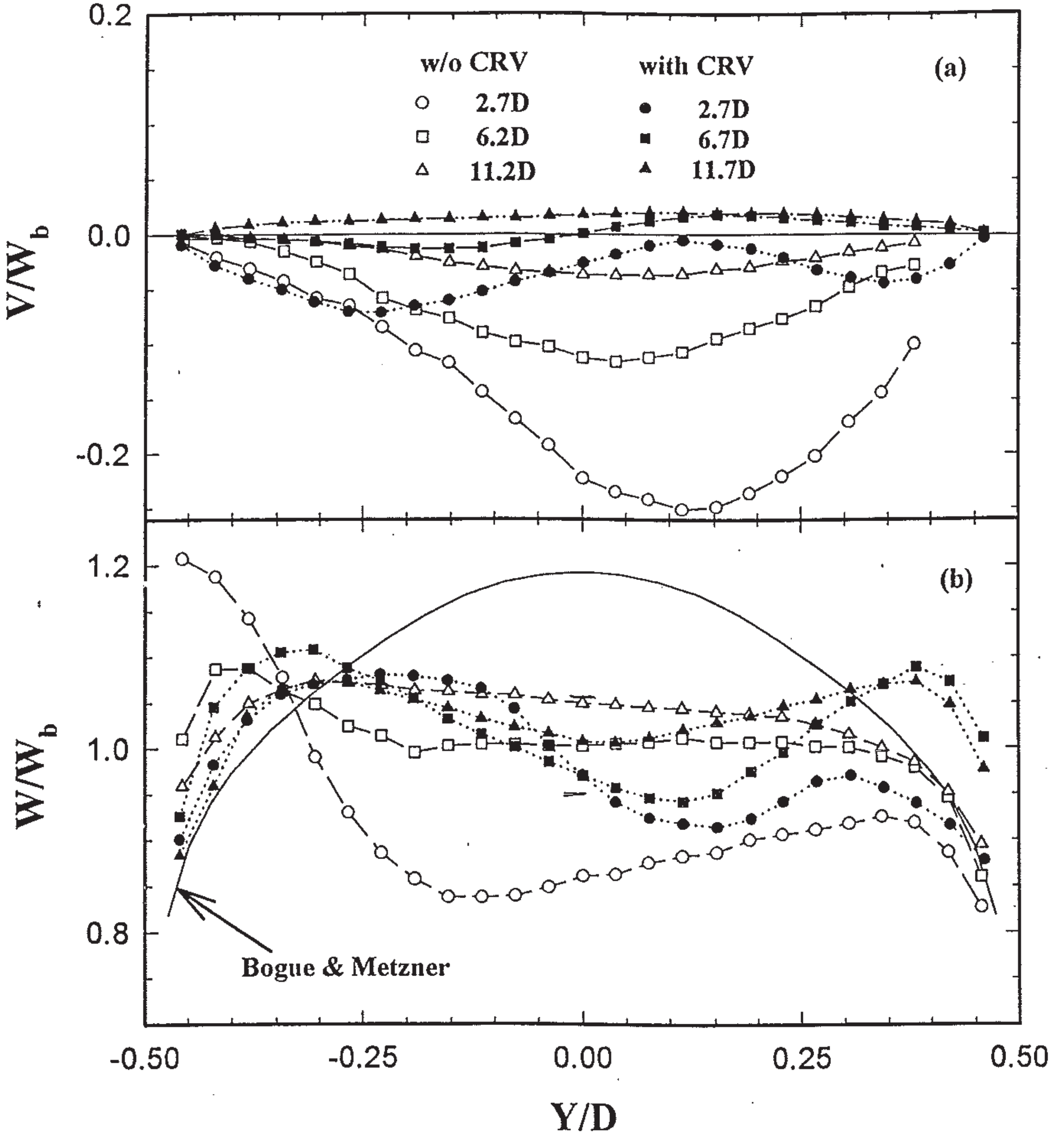

Figure 18 Comparison of Mean Velocity Profiles for Single Elbow with and without CRV for $Re = 10^5$.

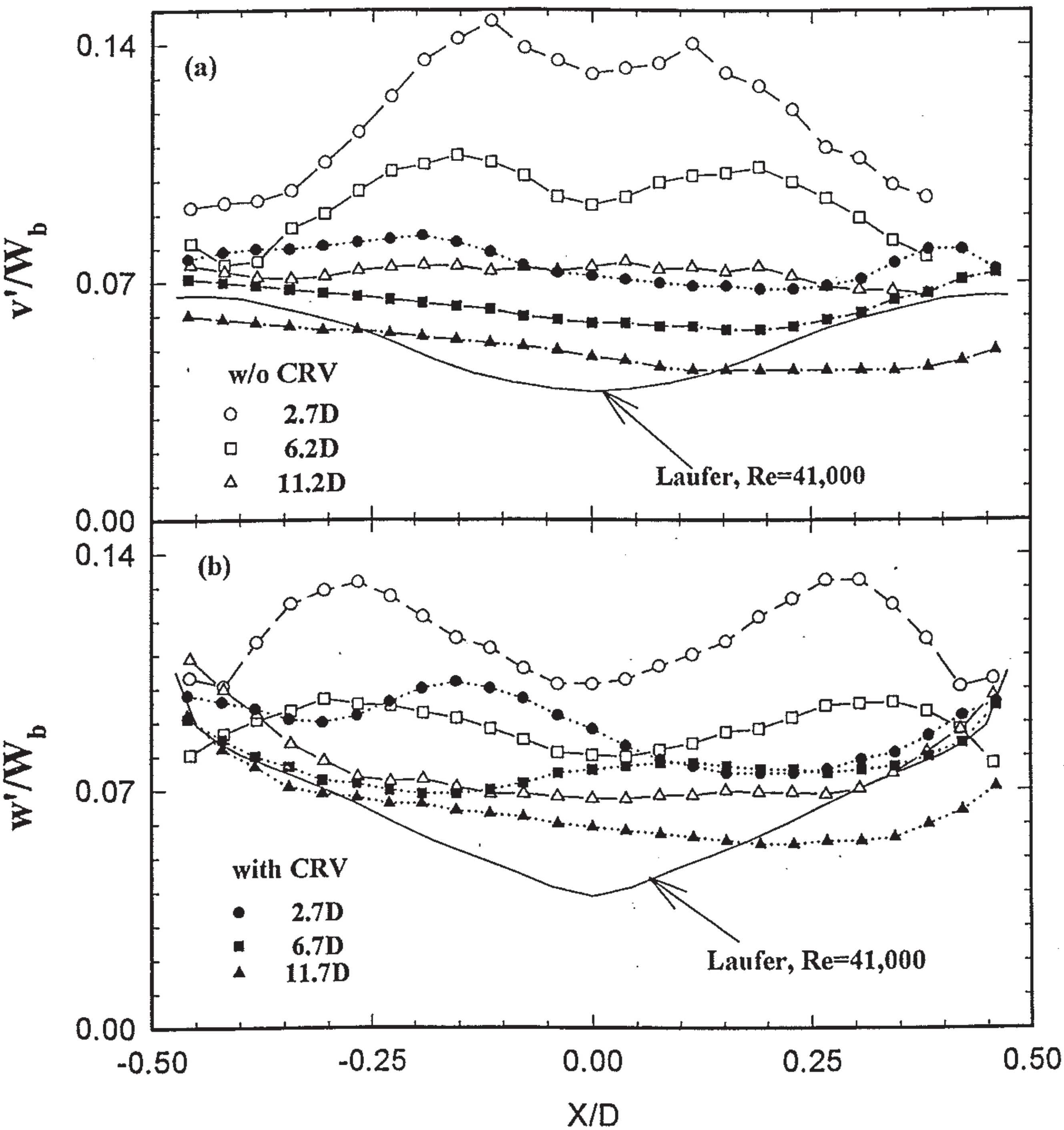

Figure 19 **Comparison of Turbulent Velocity Profiles for Single Elbow with and without CRV for $Re=10^5$.**

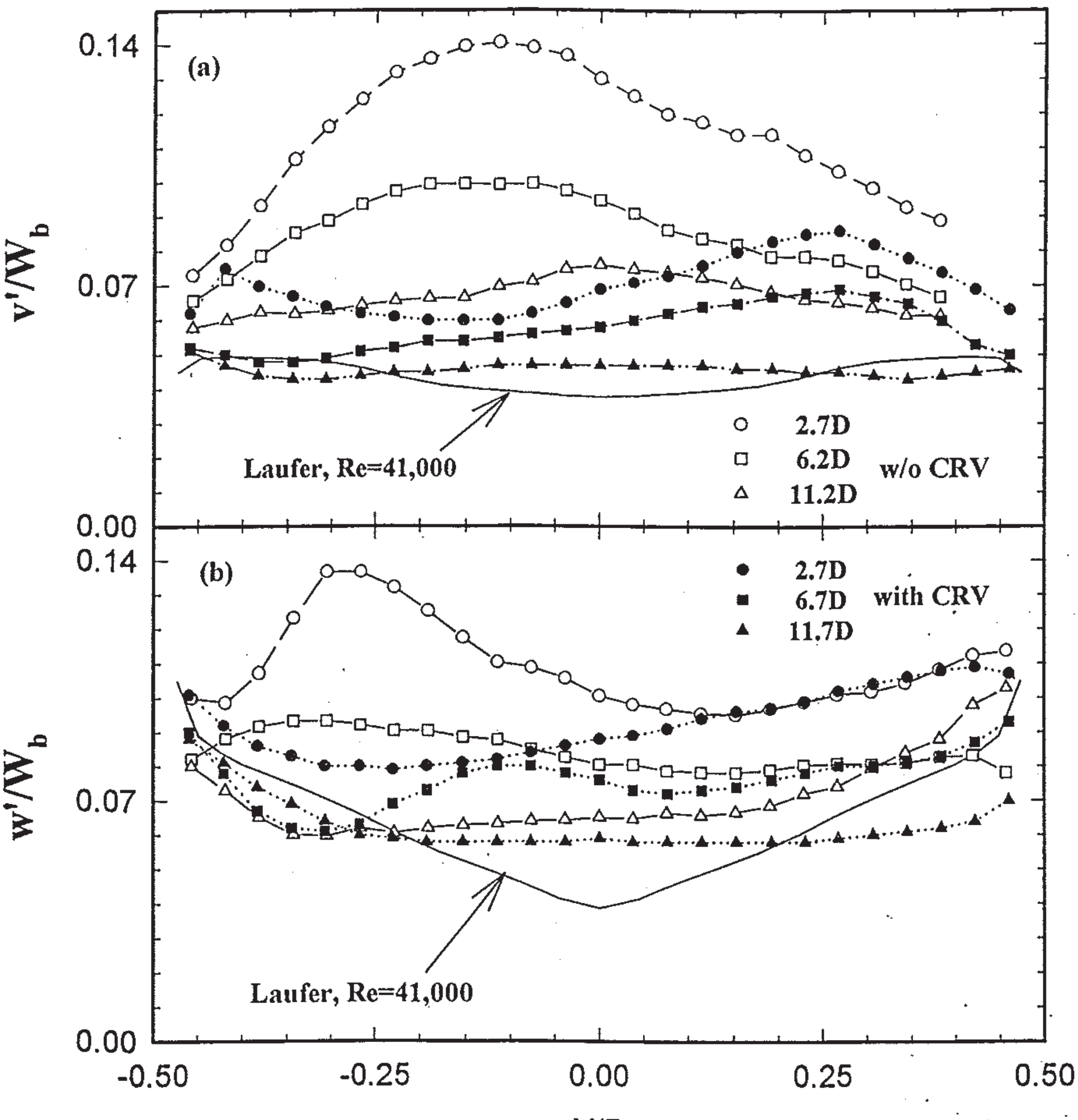

Figure 20 Comparison of Turbulent Velocity Profiles for Single Elbow with and without CRV for $Re = 10^5$.

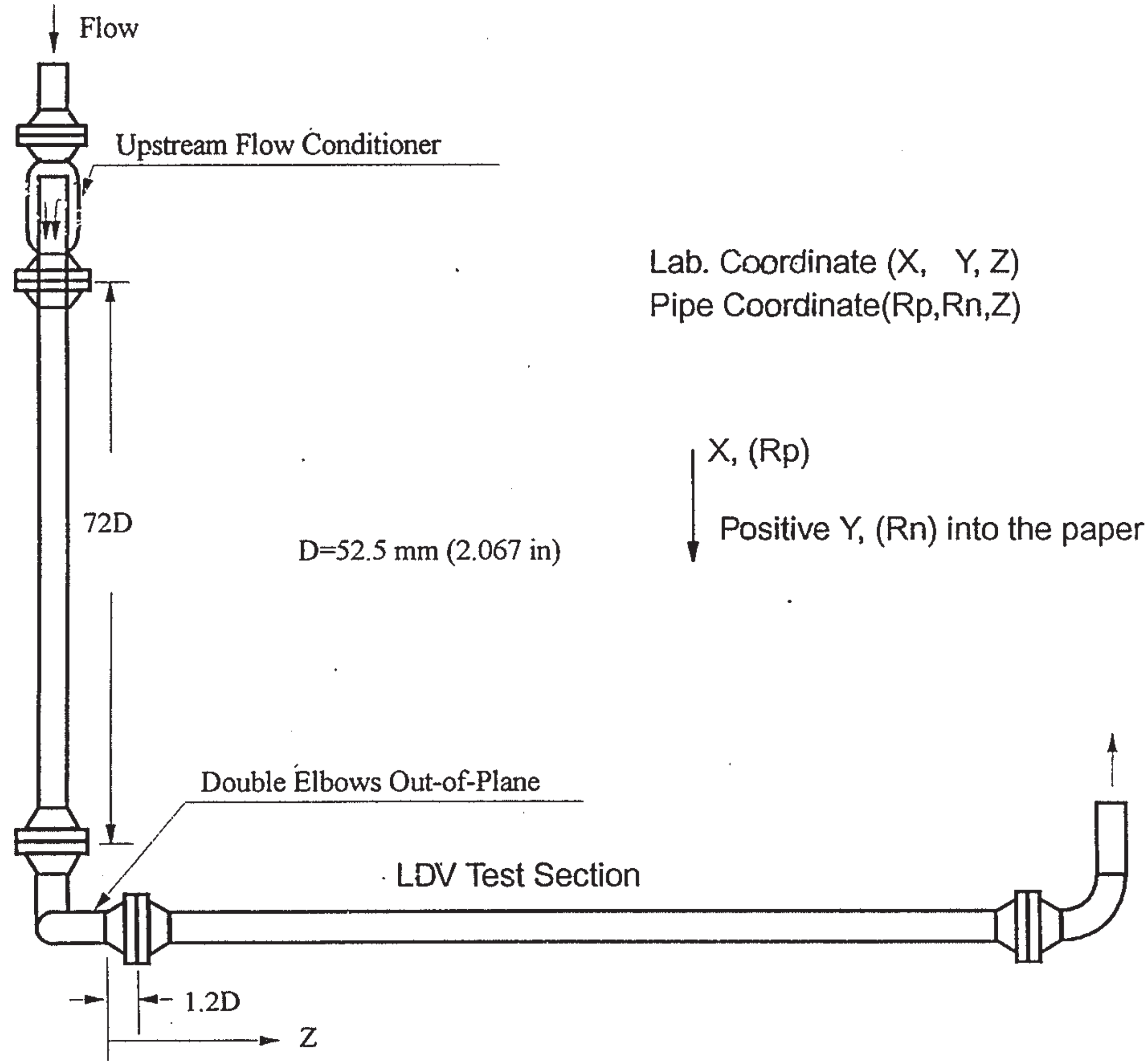

<u>Sketch 2</u> Double Elbows Out-of-Plane Configuration. (The laboratory coordinate system used is a right-handed system with Z as shown. The X coordinate is downward, and Y is into the page. The origin of the coordinate system is the centerline of the pipe in the exit plane of the second elbow. The pipe coordinates are shown in relation to the laboratory coordinates.)

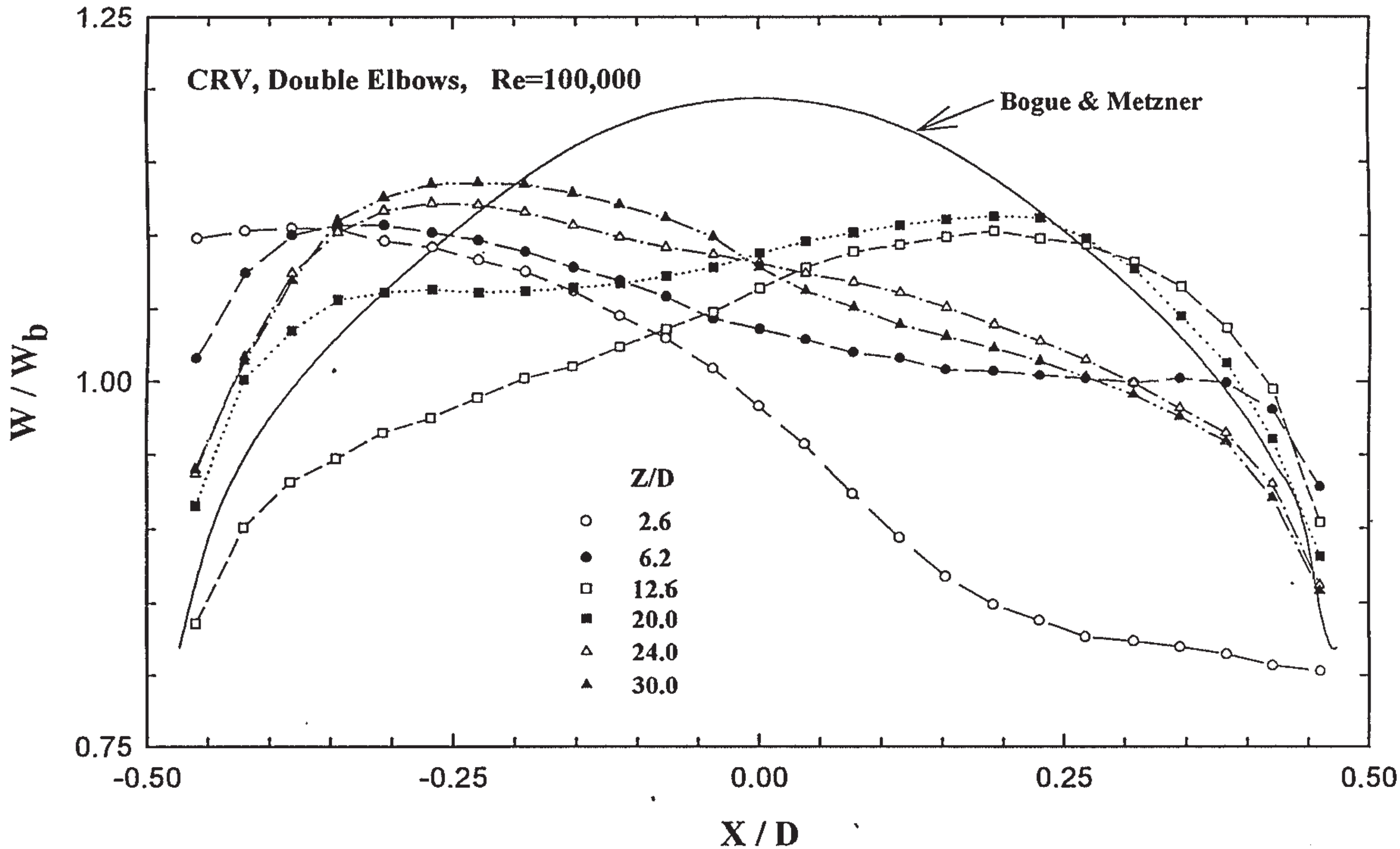

Figure 21 Profiles of the Axial Mean Velocity vs. Horizontal Radial Position at Different Downstream Locations.

WMY

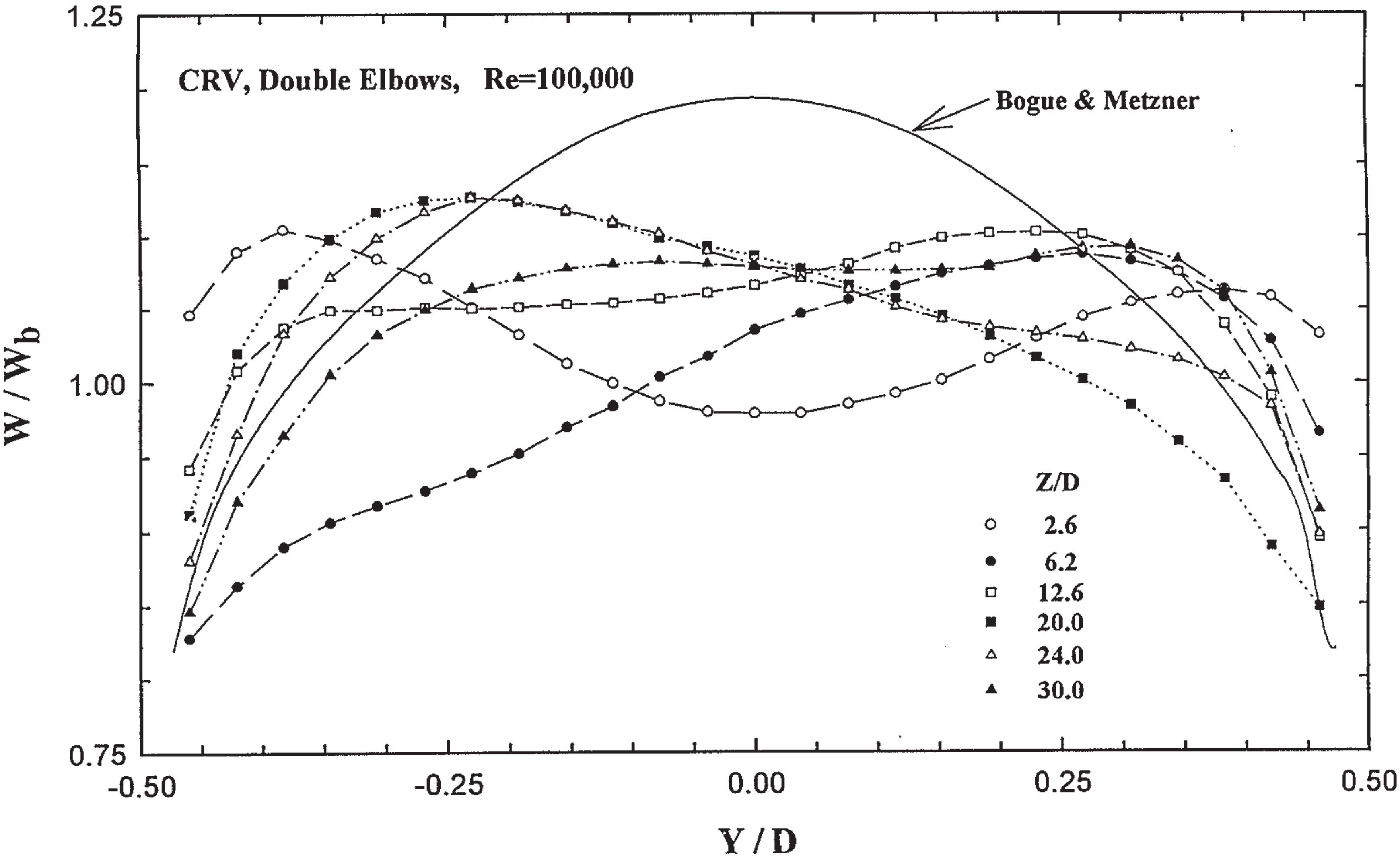

Figure 22 Profiles of the Axial Mean Velocity vs. Vertical Radial Position at Different Downstream Locations.

VMX

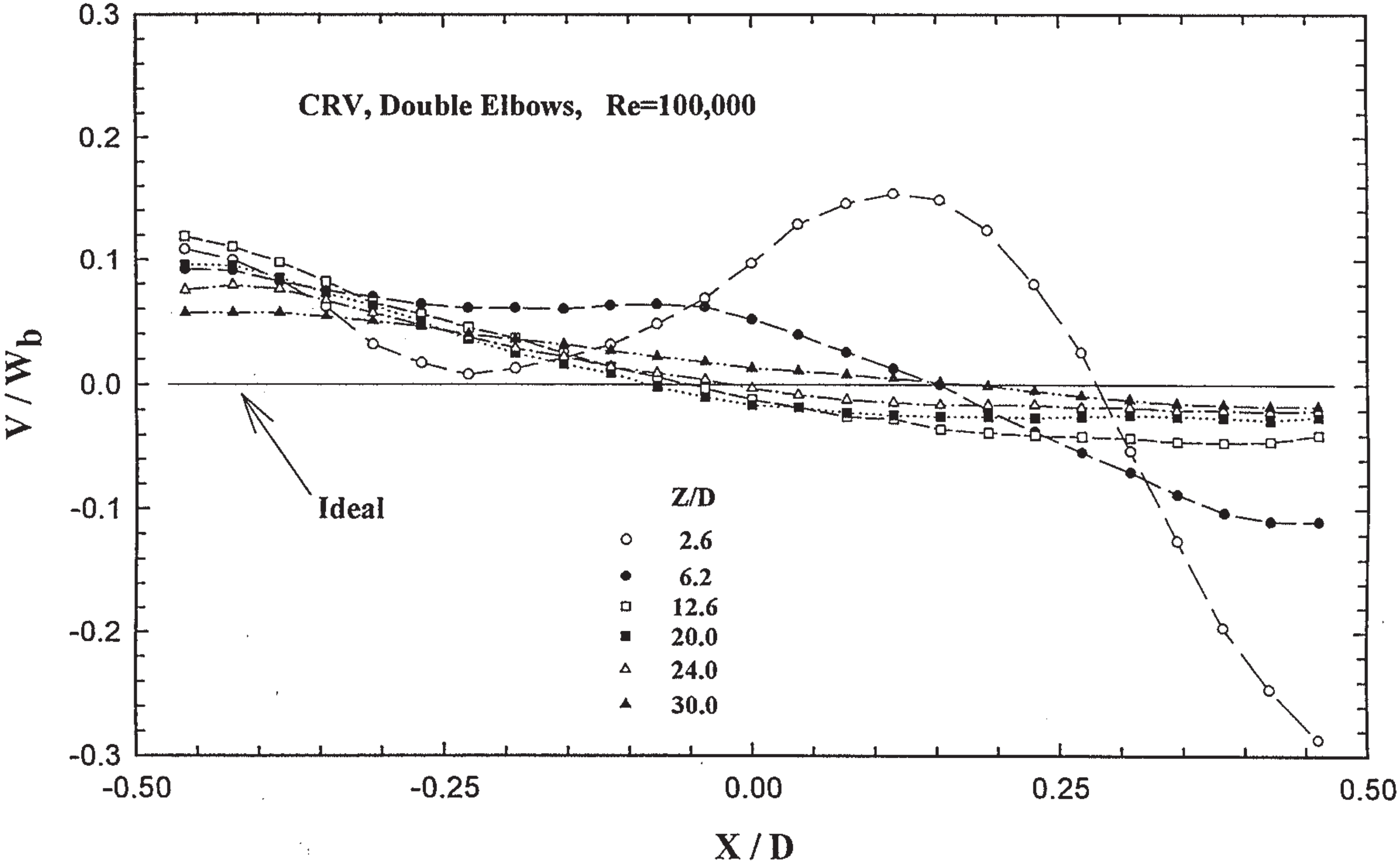

Figure 23 Profiles of the Vertical Mean Velocity vs. Horizontal Radial Position at Different Downstream Locations.

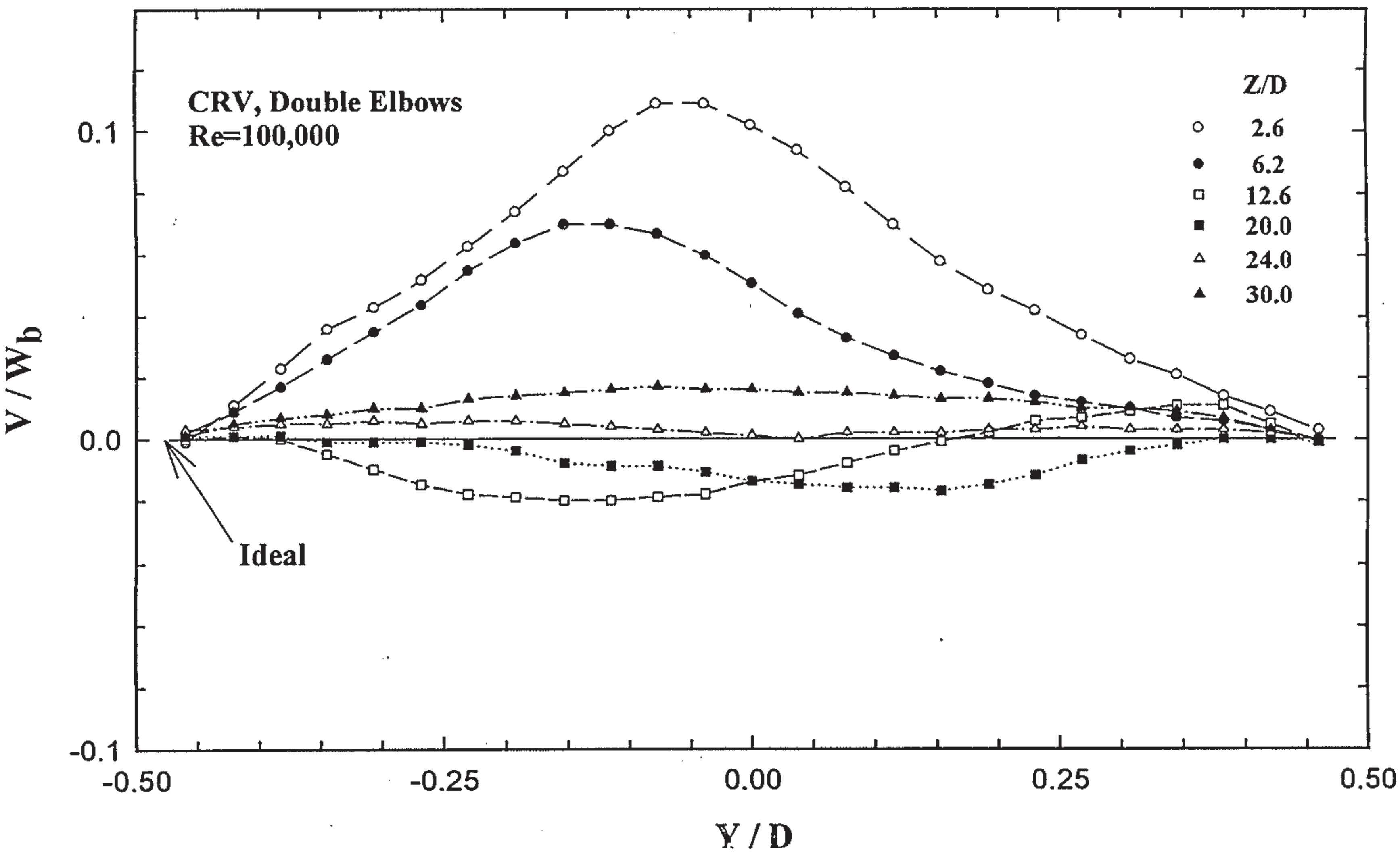

Figure 24 Profiles of the Vertical Mean Velocity vs. Vertical Radial Position at Different Downstream Locations.

WTX

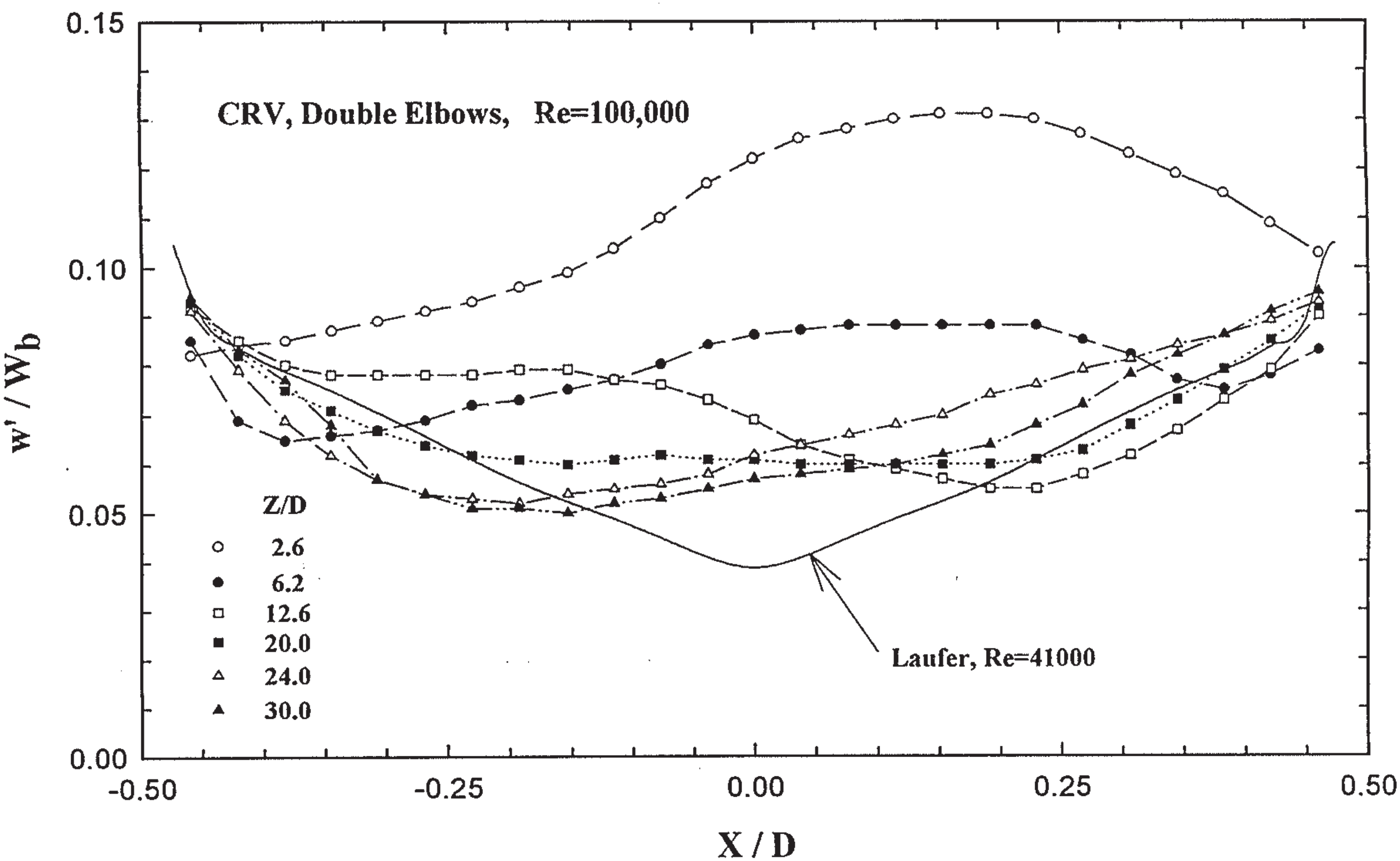

Figure 25 Profiles of the Axial Turbulent Velocity vs. Horizontal Radial Position at Different Downstream Locations.

WTY

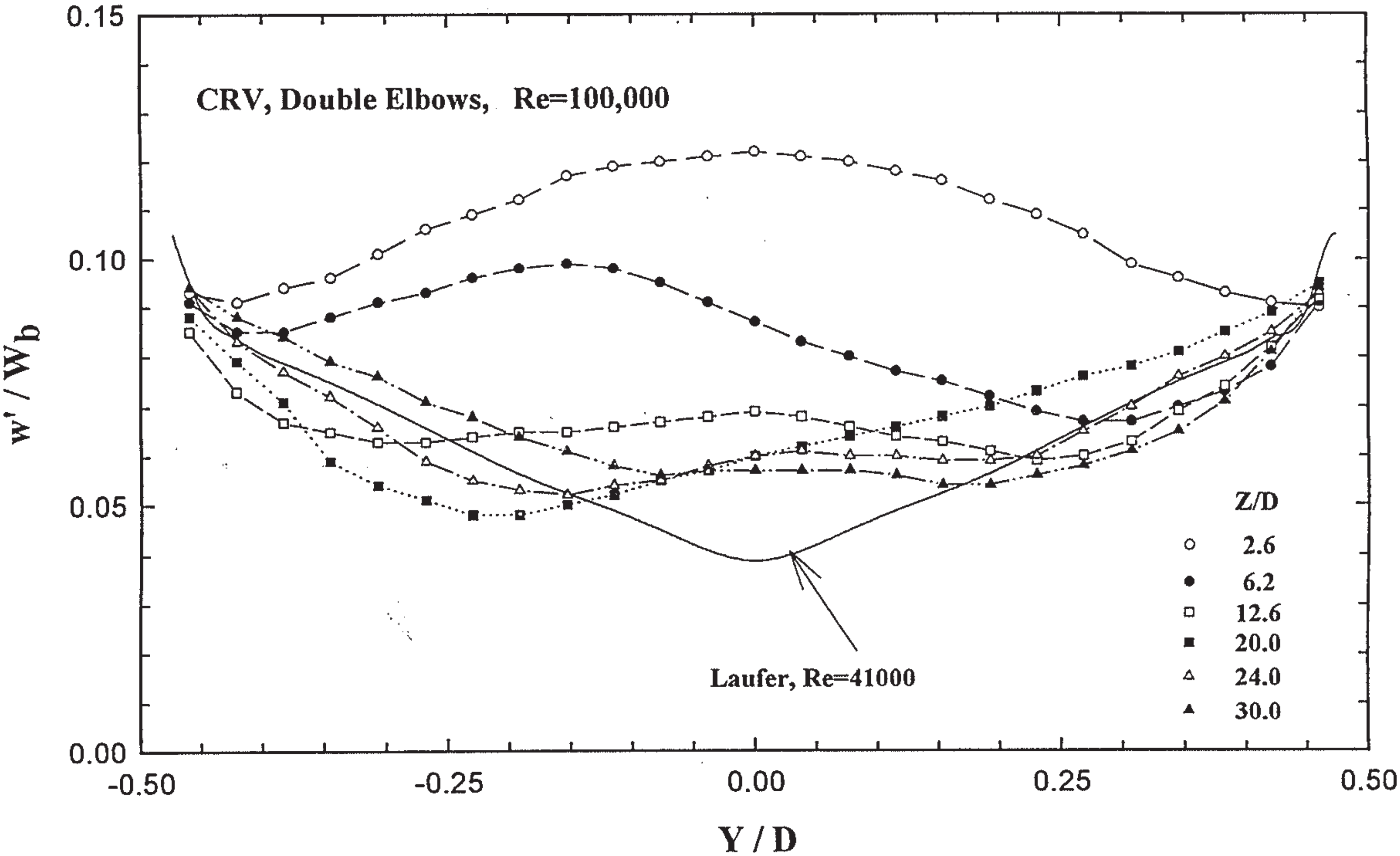

<u>Figure 26</u> Profiles of the Axial Turbulent Velocity vs. Vertical Radial Position at Different Downstream Locations.

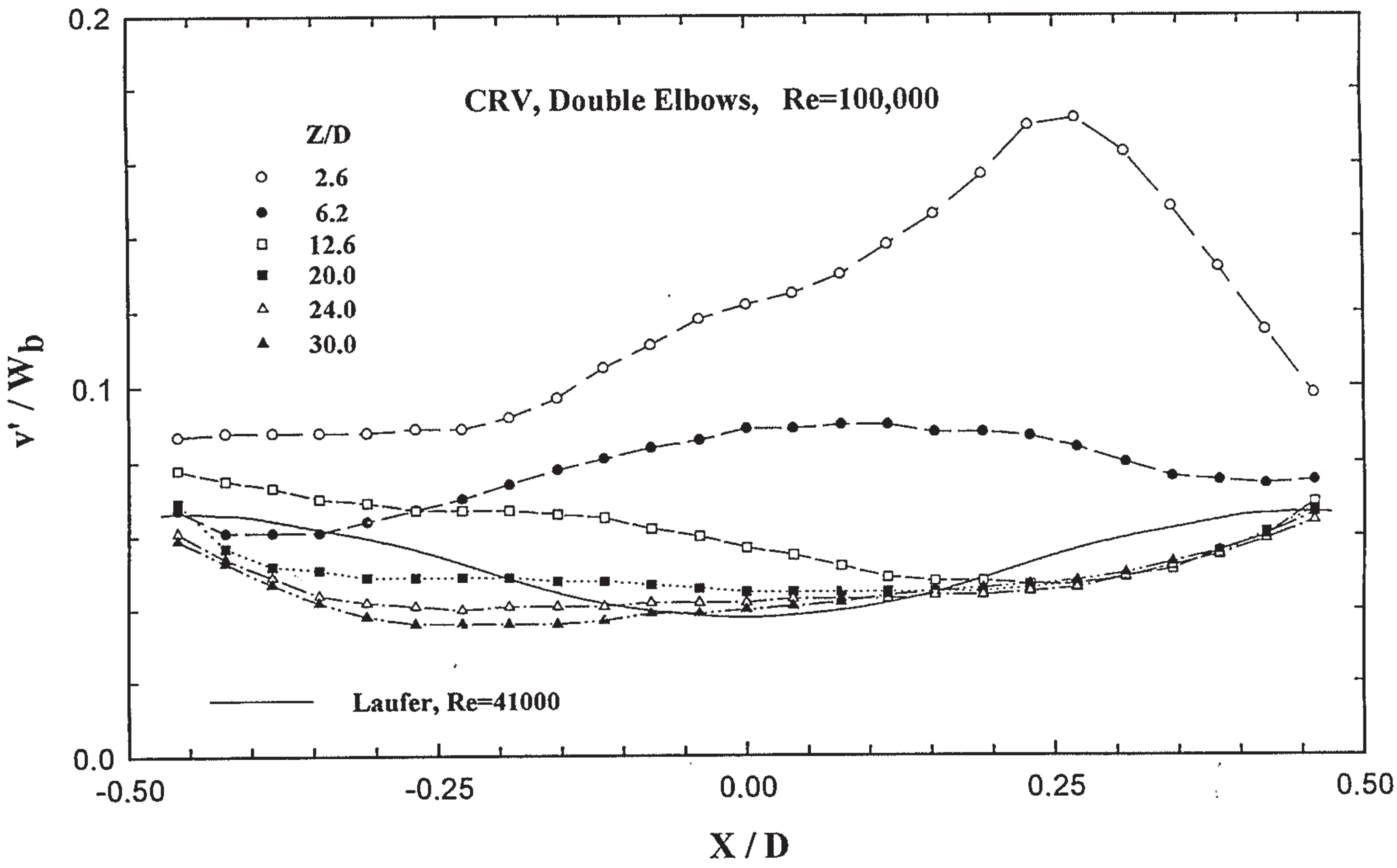

Figure 27 Profiles of the Vertical Turbulent Velocity vs. Horizontal Radial Position at Different Downstream Locations.

VTY

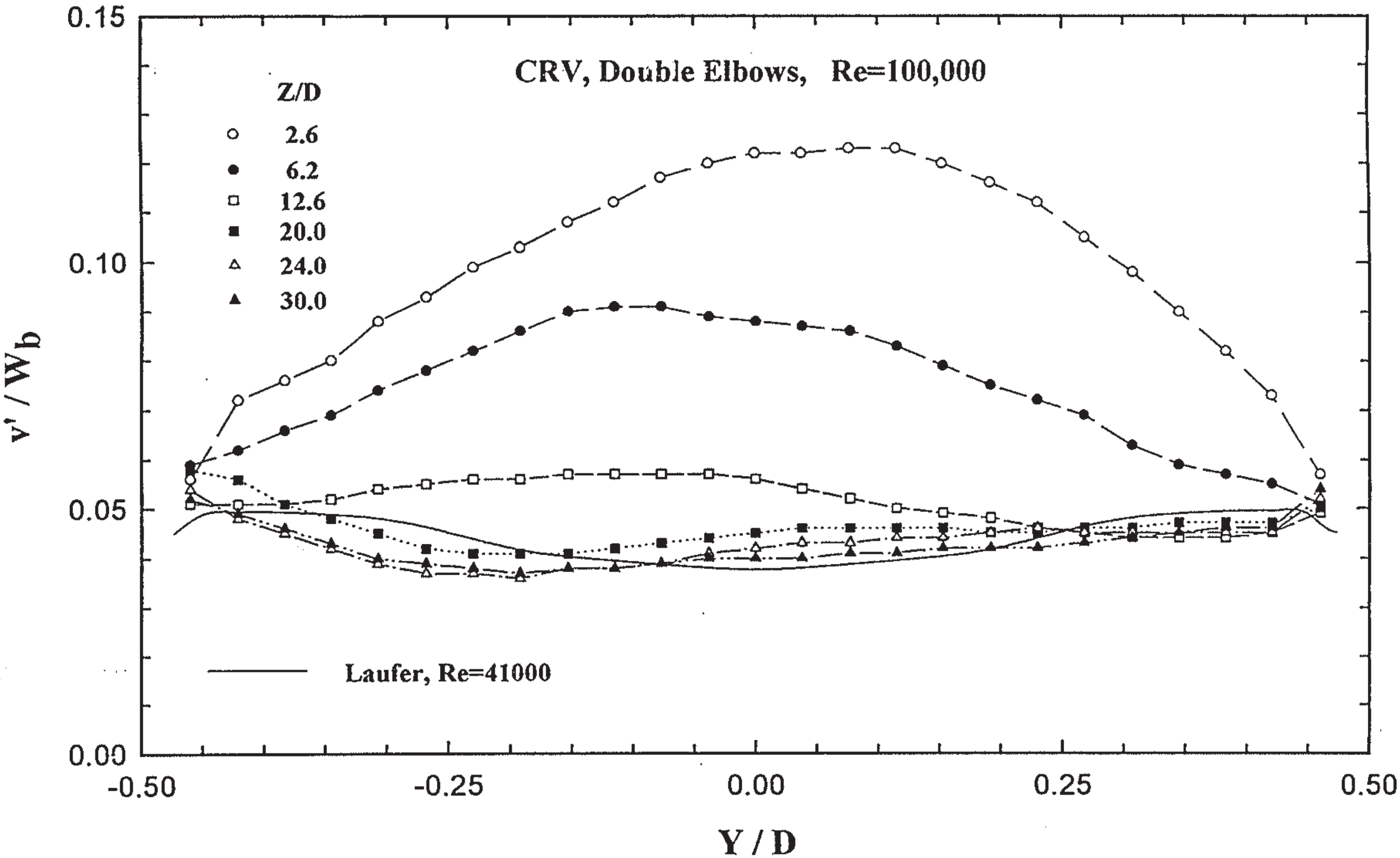

Figure 28 Profiles of the Vertical Turbulent Velocity vs. Vertical Radial Position at Different Downstream Locations.

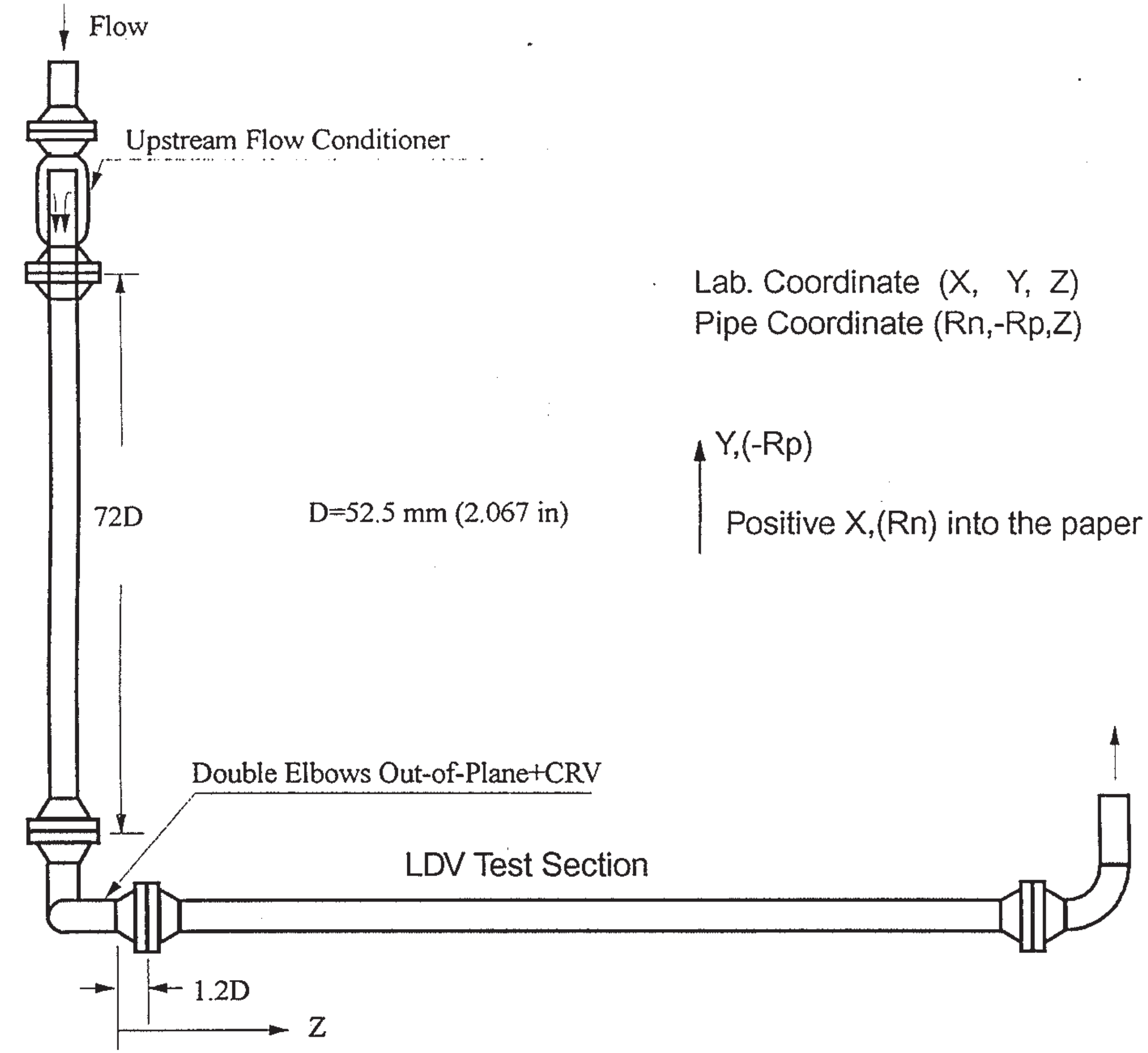

<u>Sketch 3</u> Double Elbows Out-of-Plane Configuration with the CRV installed. The relationships are shown between the laboratory coordinates and the pipe coordinates.

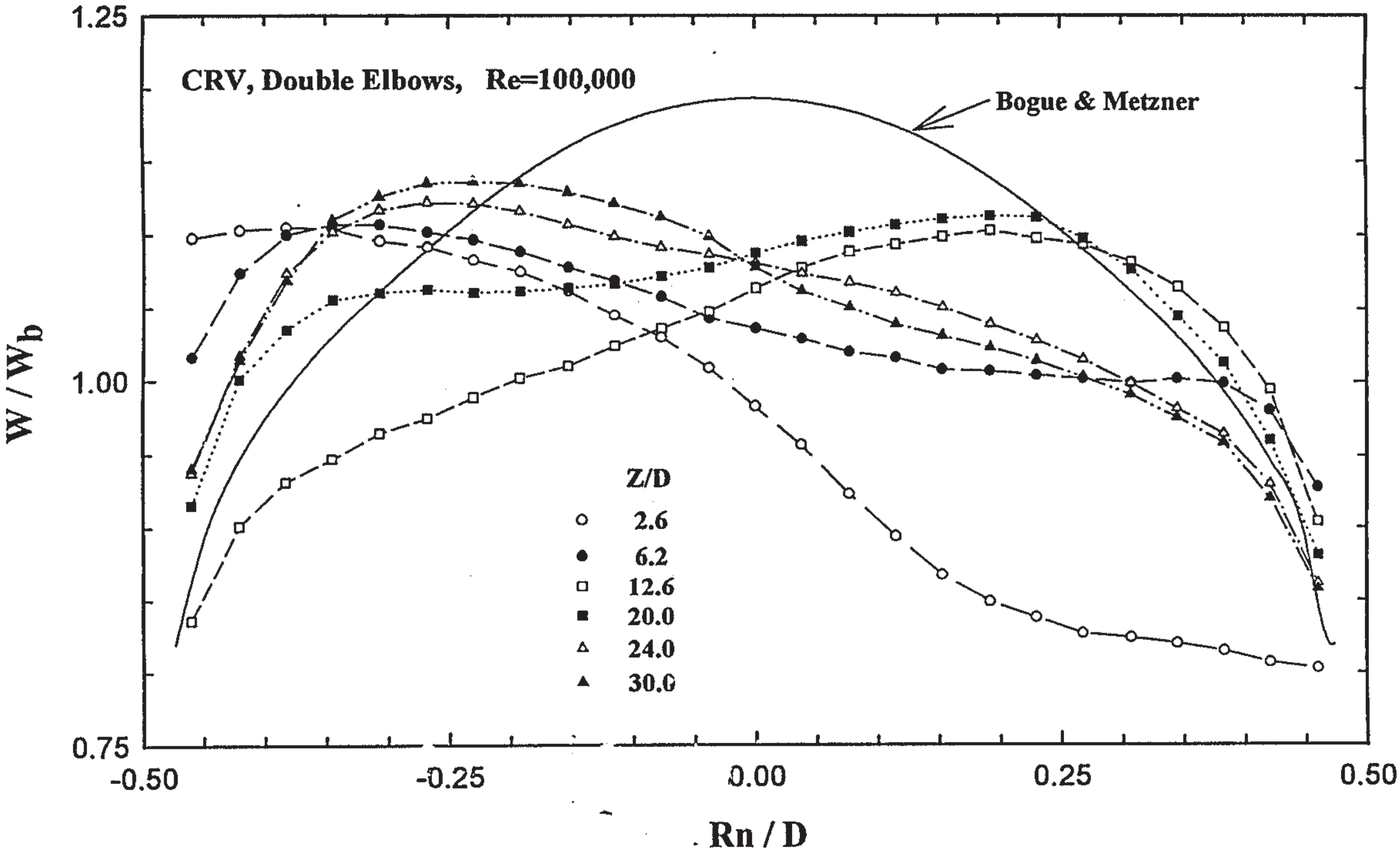

Figure 29 Profiles of the Axial Mean Velocity vs. Normal Radial Position, Rn at Different Downstream Locations.

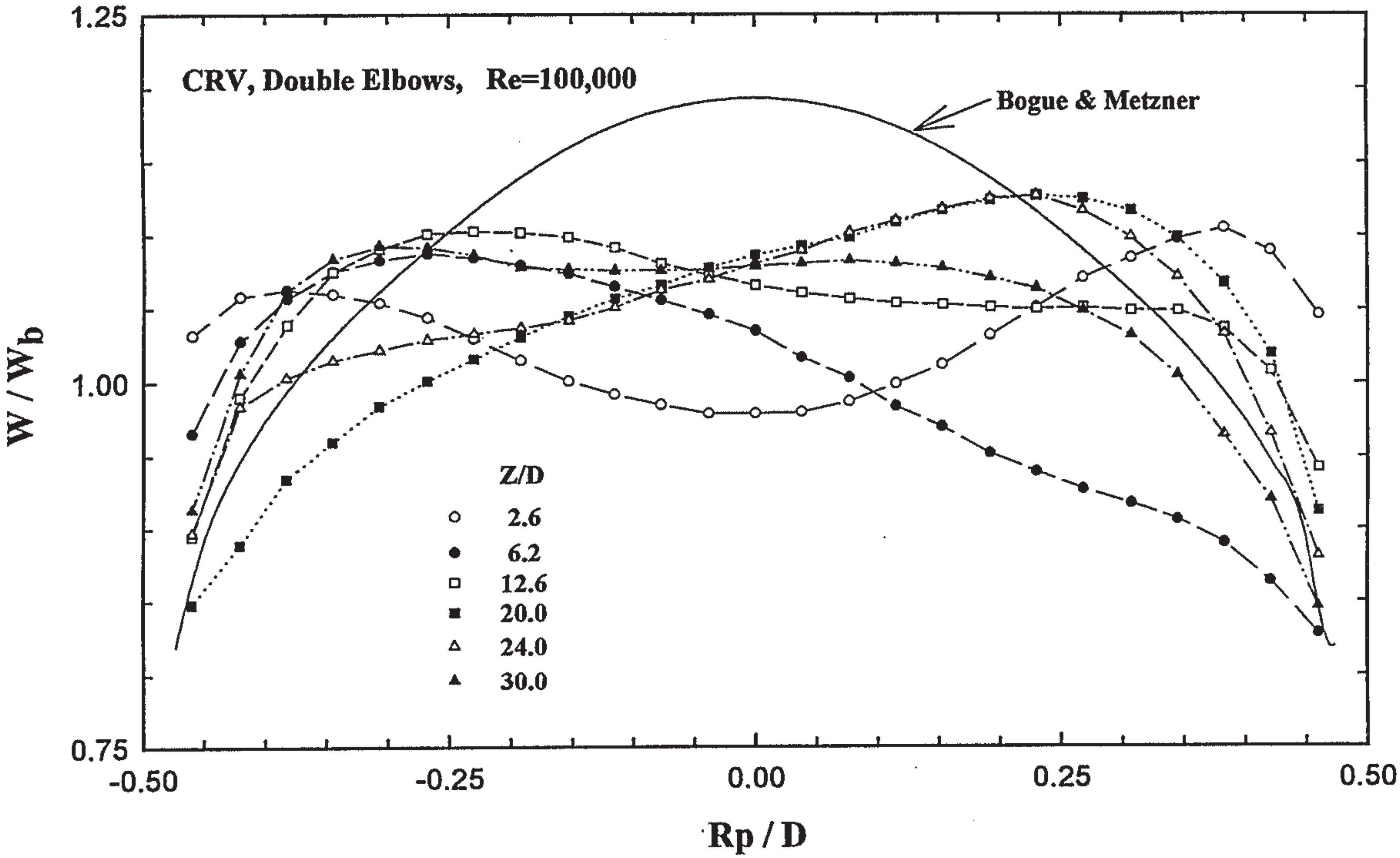

Figure 30 Profiles of the Axial Mean Velocity vs. In-plane Radial Position, Rp at Different Downstream Locations.

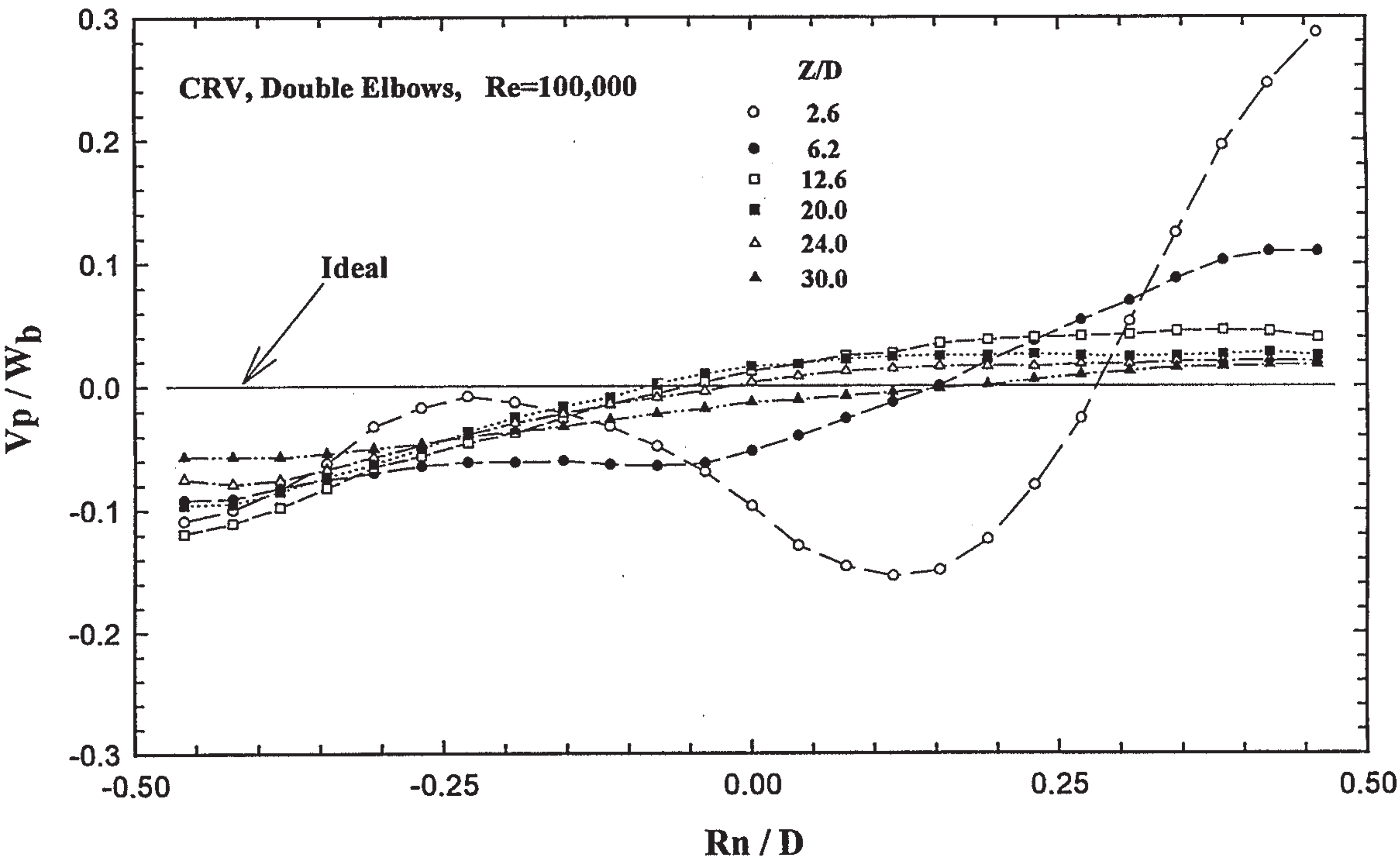

Figure 31 Profiles of the Transverse Mean Velocity, Vp vs. Normal Radial Position, Rn at Different Downstream Locations.

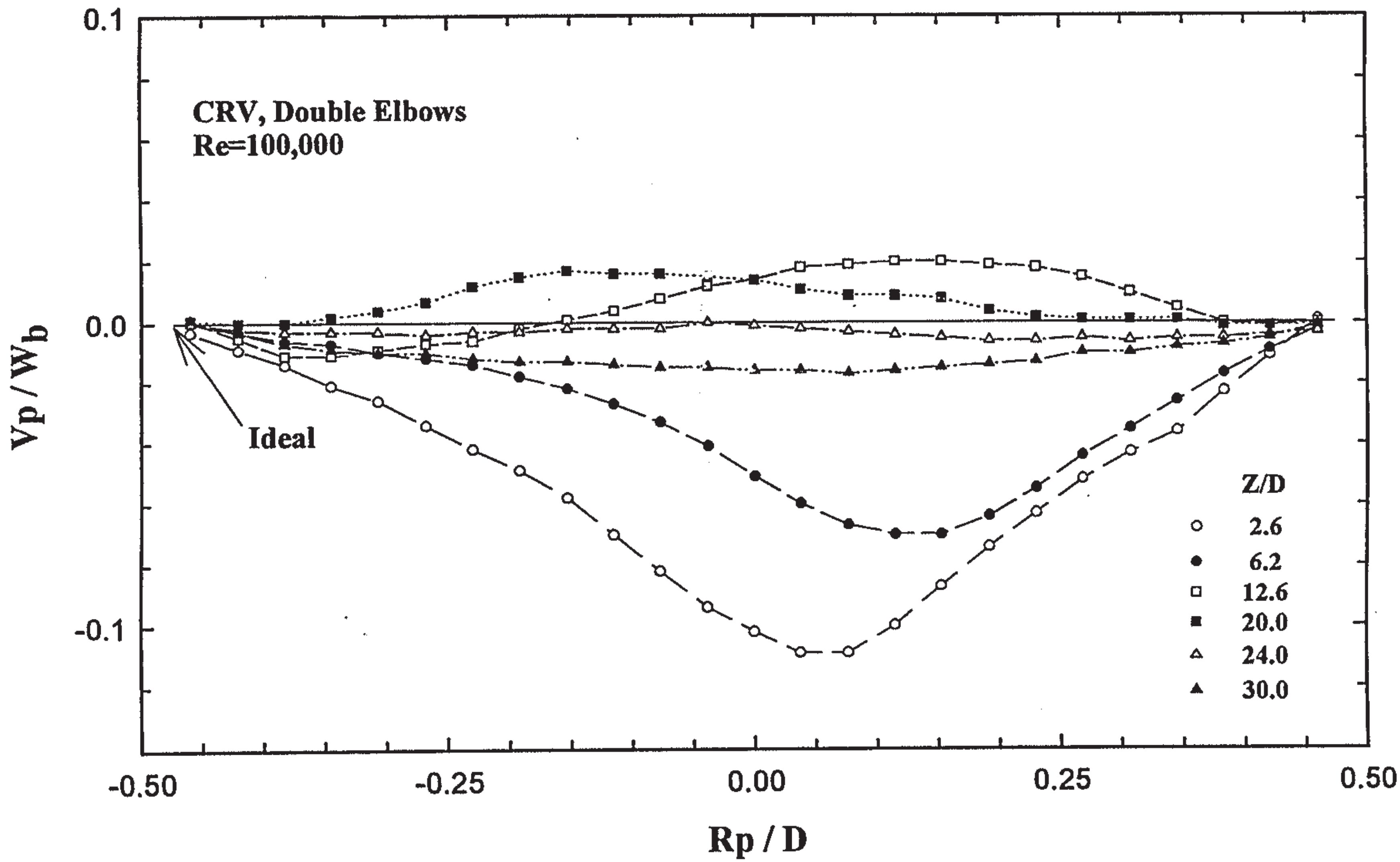

Figure 32 Profiles of the Transverse Mean Velocity vs. In-plane Radial Position, Rp at Different Downstream Locations.

WTNC

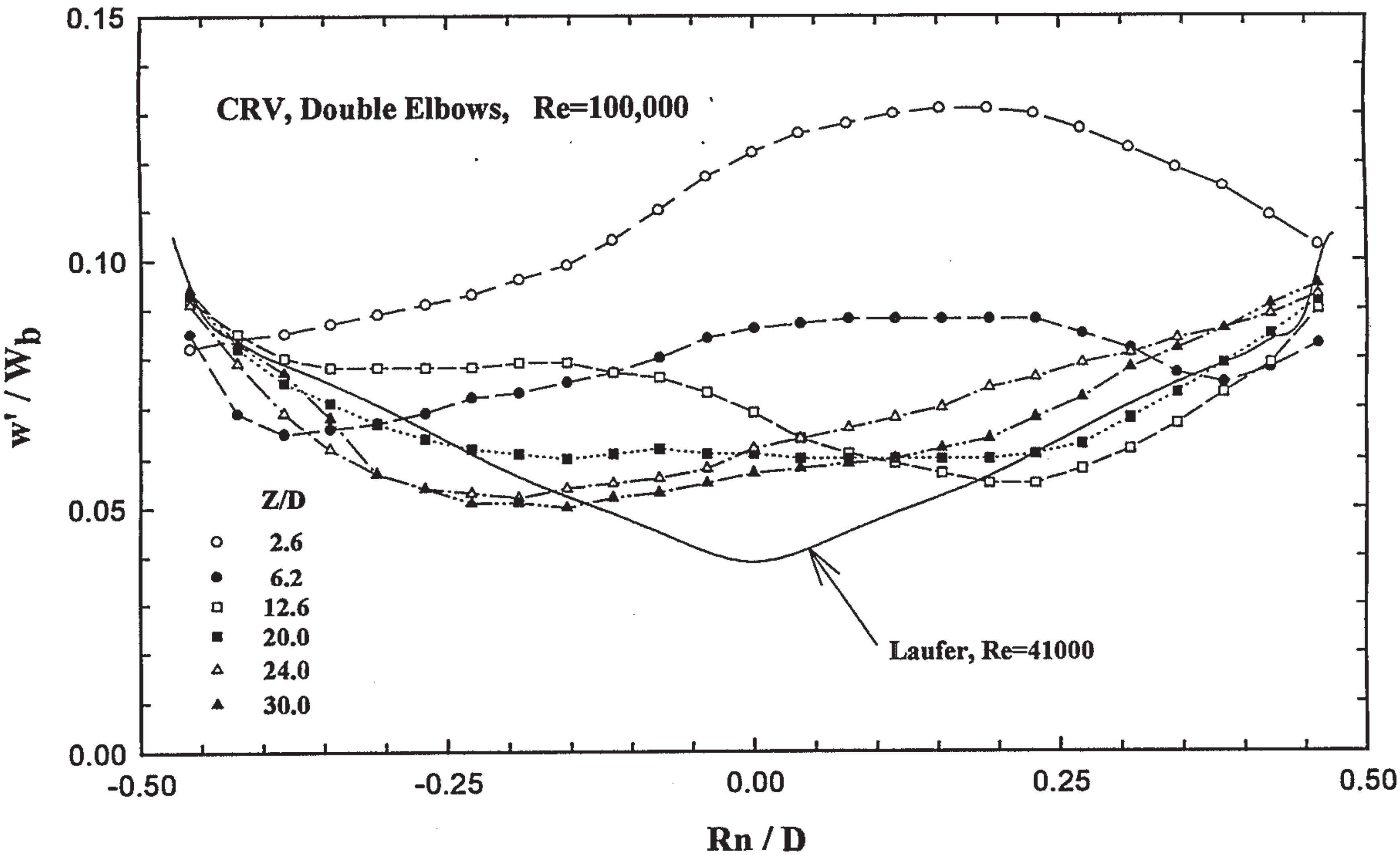

<u>Figure 33</u> Profiles of the Axial Turbulent Velocity vs. Normal Radial Position, Rn at Different Downstream Locations.

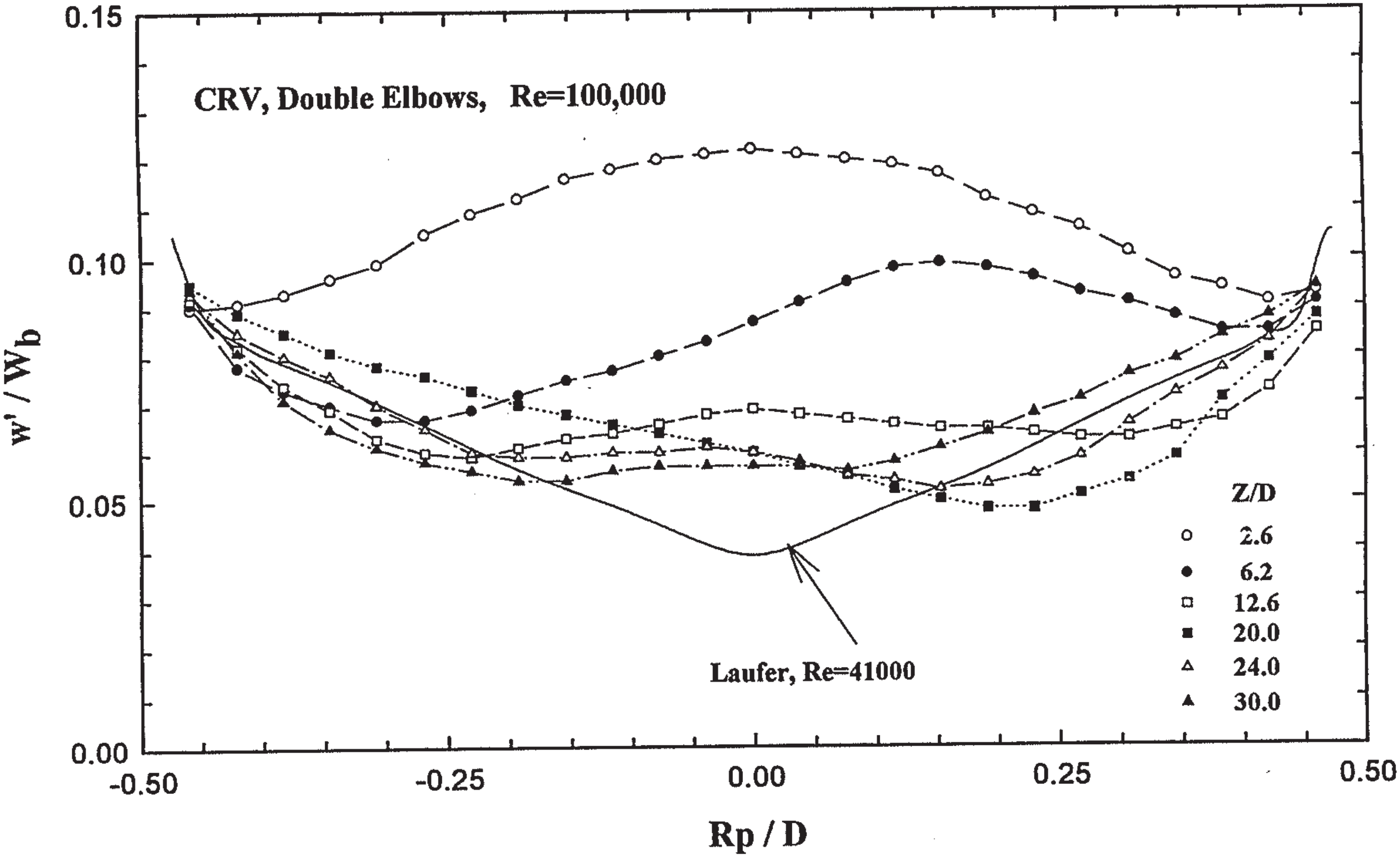

<u>Figure 34</u> **Profiles of the Axial Turbulent Velocity vs. In-plane Radial Position, Rp at Different Downstream Locations.**

VpTNC

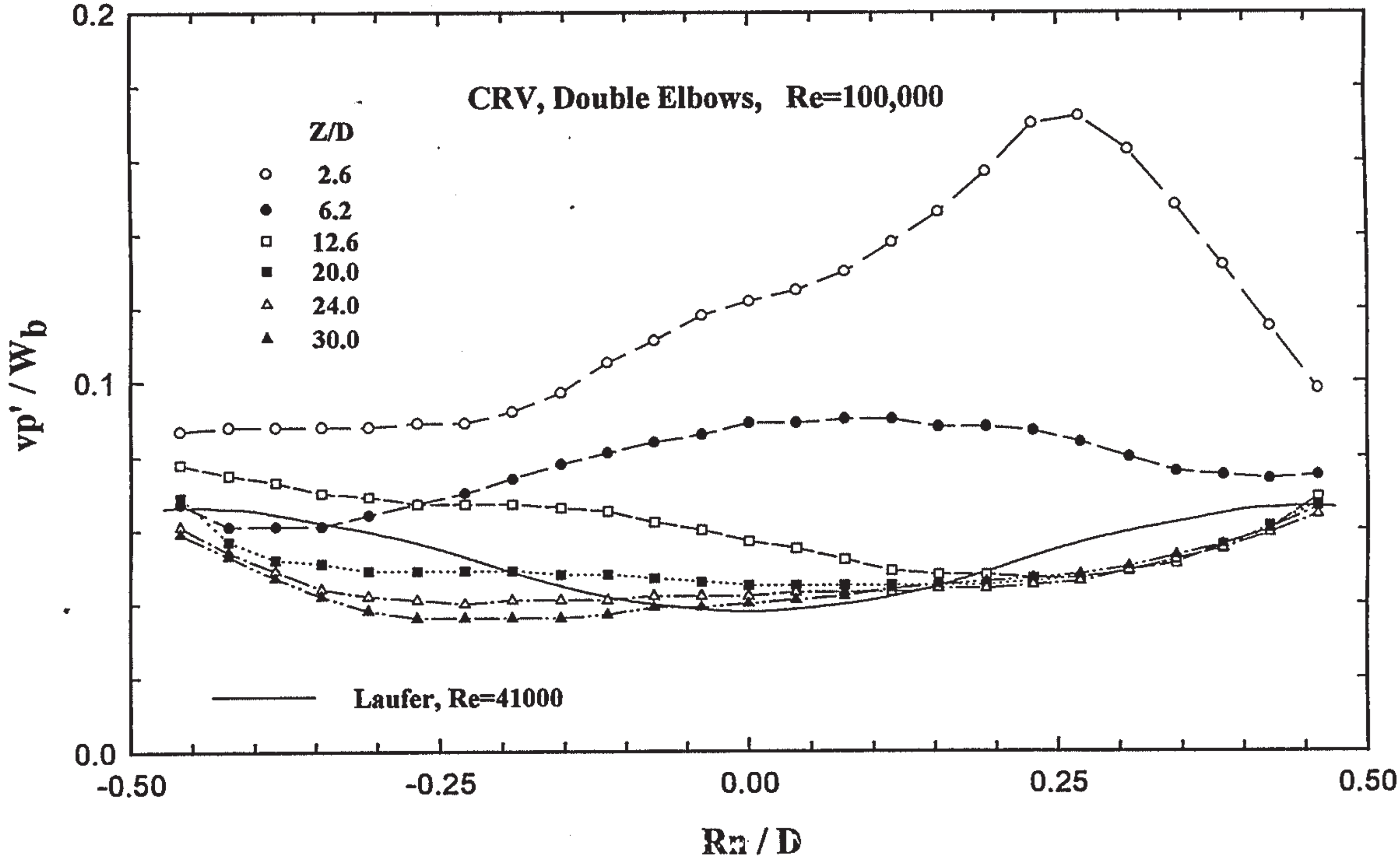

Figure 35 Profiles of the Transverse Turbulent Velocity vs. Normal Radial Position, Rn at Different Downstream Locations.

VpTPC

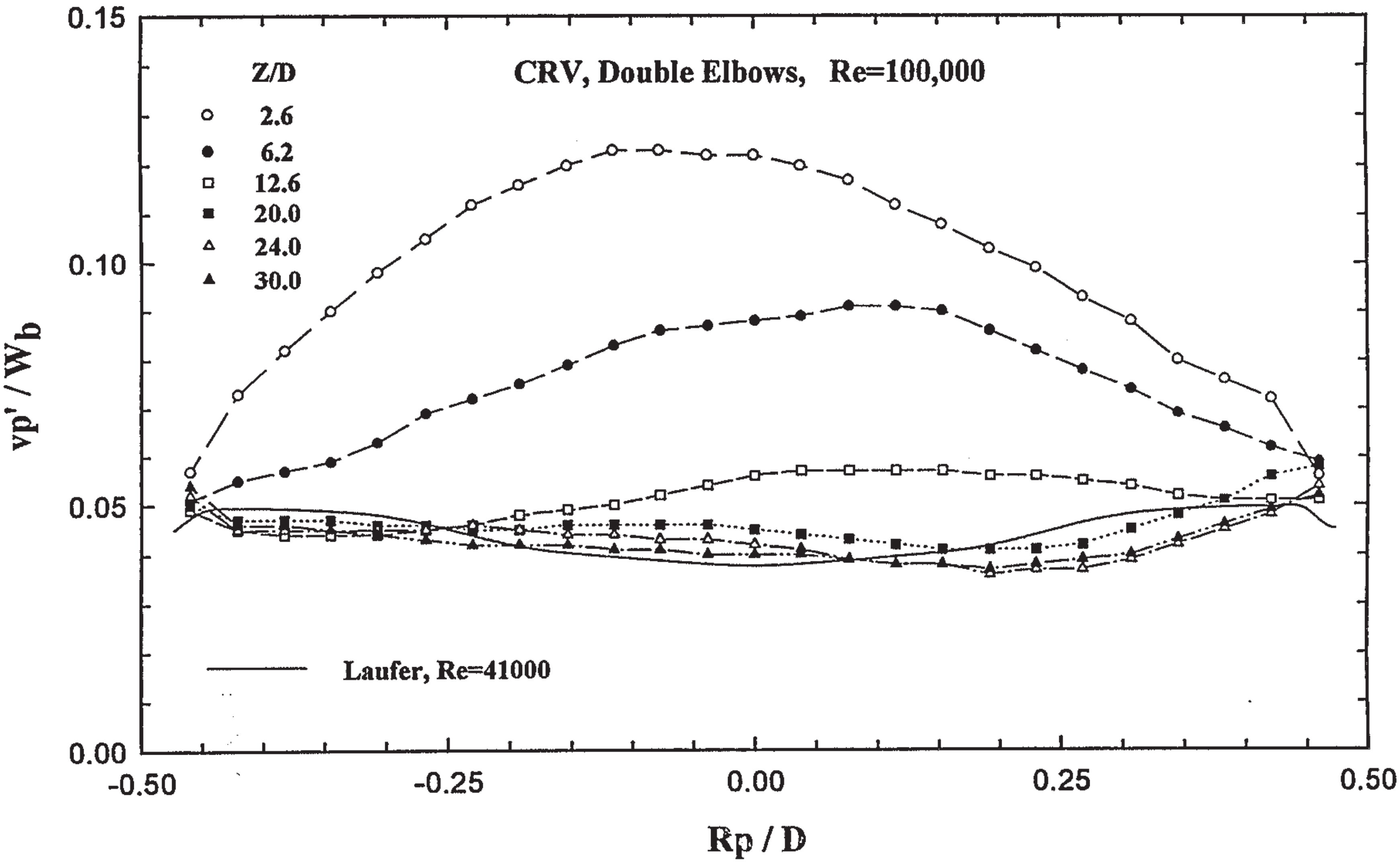

Figure 36 Profiles of the Transverse Turbulent Velocity, Vp vs. In-plane Radial Position, Rp at Different Downstream Locations.

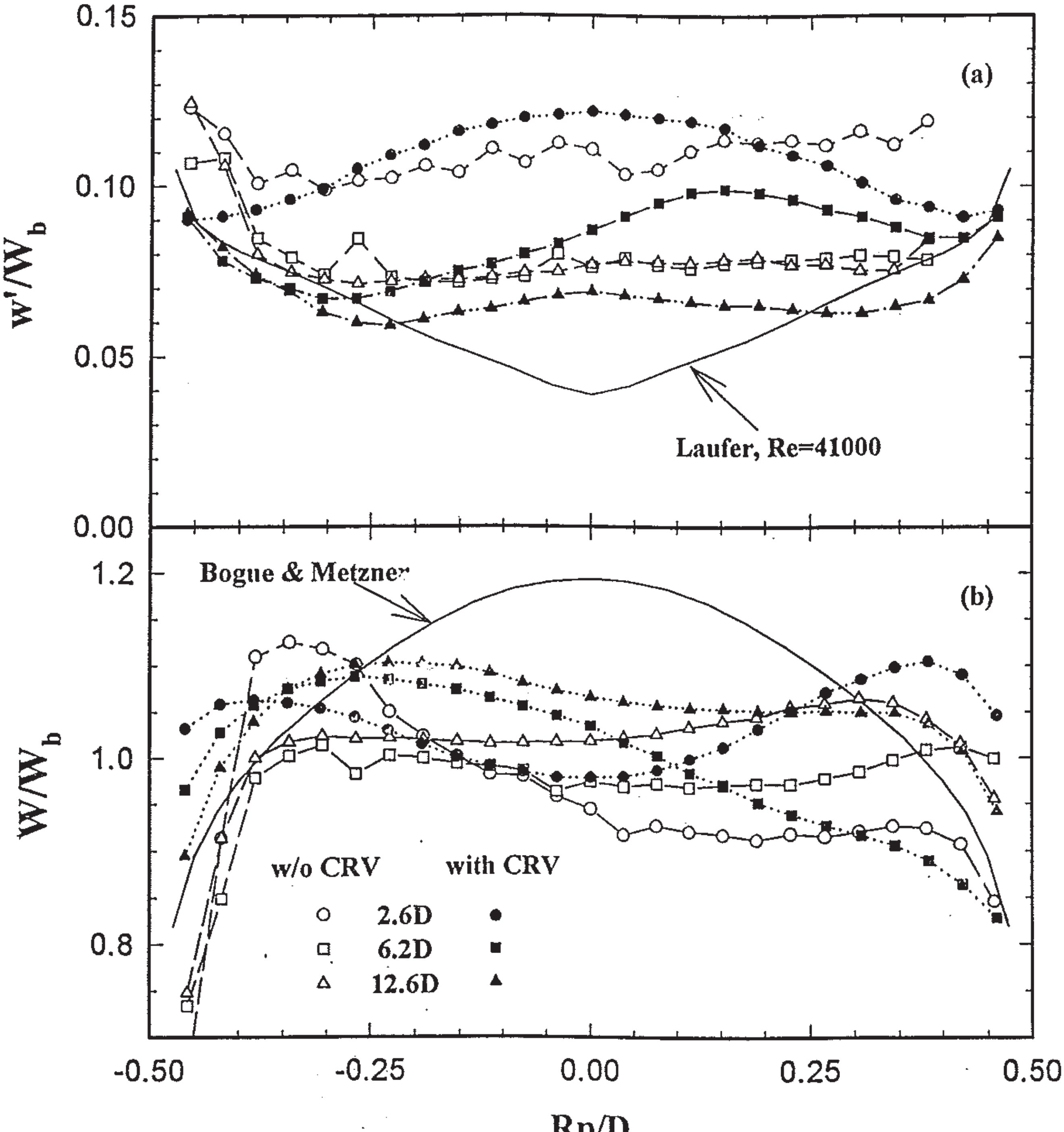

__Figure 37__ **Comparison of the Profiles of the Mean and Turbulent Axial Velocity for Double Elbows with and without CRV for Re=10^5.**

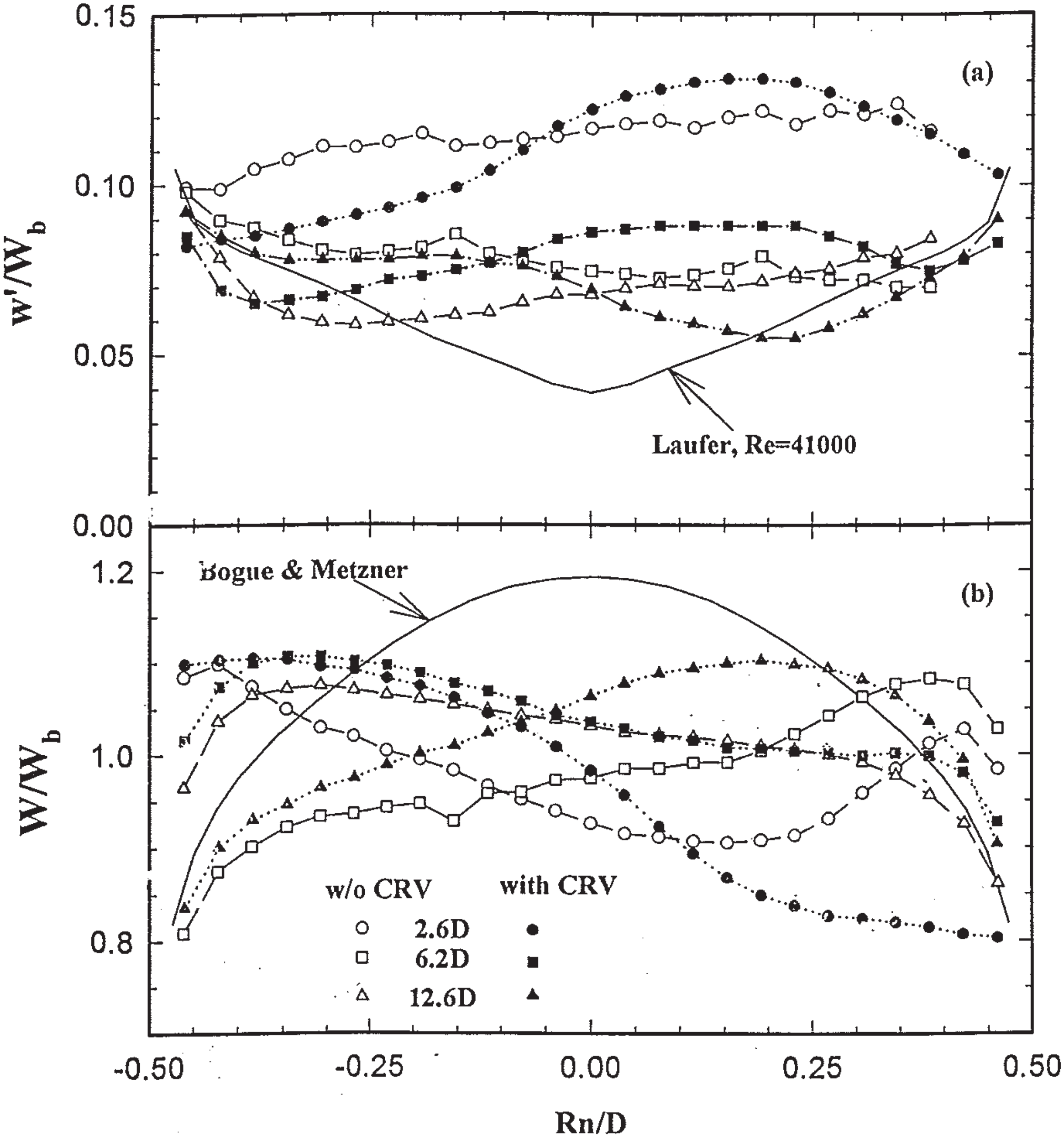

Figure 38 Comparison of the Profiles of the Mean and Turbulent Axial Velocity for Double Elbows with and without CRV for $Re = 10^5$.

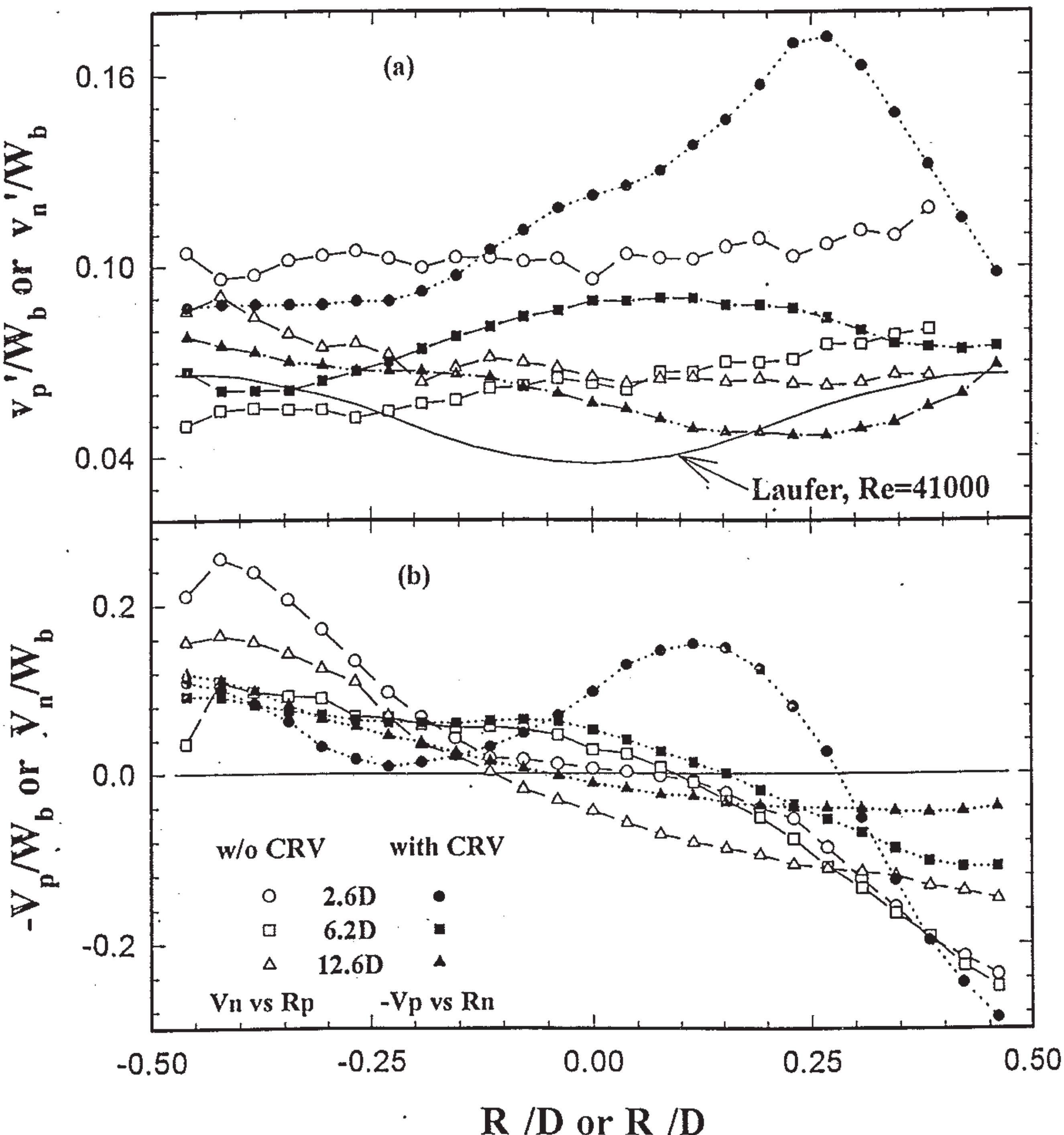

<u>Figure 39</u> Comparison of the Profiles of the Transverse (swirl) Mean and Turbulent Velocity for Double Elbows with and without CRV for Re=10^5.